Title	PAPR Constrained Power Allocation for Multi-Carrier Transmission in Multiuser SIMO Communications
Author(s)	Trevor, Valtteri; Tolli, Anti; Matsumoto, Tad
Citation	IEEE Transactions on Wireless Communications, 15(4): 2458-2473
Issue Date	2015-11-30
Type	Journal Article
Text version	author
URL	http://hdl.handle.net/10119/13001
Rights	This is the author's version of the work. Copyright (C) 2015 IEEE. IEEE Transactions on Wireless Communications, 15(4), 2015, pp.2458-2473. DOI:10.1109/TWC.2015.2504368. Personal use of this material is permitted. Permission from IEEE must be obtained for all other uses, in any current or future media, including reprinting/republishing this material for advertising or promotional purposes, creating new collective works, for resale or redistribution to servers or lists, or reuse of any copyrighted component of this work in other works.
Description	

PAPR Constrained Power Allocation for Multi-Carrier Transmission in Multiuser SIMO Communications

Valtteri Tervo*, *Member, IEEE,* Antti Tölli, *Senior Member, IEEE,* Tad Matsumoto, *Fellow, IEEE*

***Abstract*—Peak-to-average power ratio (PAPR) constrained power allocation for multicarrier transmission in multiuser single-input multiple-output (SIMO) communications is considered in this paper. Reducing the PAPR in any transmission system is beneficial because it allows the use of inexpensive, energy-efficient power amplifiers. In this paper, we formulate a power allocation problem for single-carrier (SC) frequency division multiple access (FDMA) and orthogonal FDMA (OFDMA) transmission with instantaneous PAPR constraints. Moreover, a statistical approach is considered in which the power variance of the transmitted waveform is controlled. The constraints for the optimization problems are derived as a function of transmit power allocation and two successive convex approximations (SCAs) are derived for each of the constraints based on a change of variables (COV) and geometric programming (GP). In addition, the optimization problem is constrained by a user-specific quality of service (QoS) constraint. Hence, the proposed power allocation strategy jointly takes into account the channel quality and the PAPR characteristics of the power amplifier. The numerical results show that the proposed power allocation strategy can significantly improve the transmission efficiency of power-limited users. Therefore, it is especially beneficial for improving the performance for cell edge users.**

***Index Terms*—Power minimization, soft interference cancellation, MMSE receiver, multiuser detection, PAPR reduction**

I. INTRODUCTION

Single-carrier (SC) frequency division multiple access (FDMA) [1] has been selected as the uplink transmission scheme for the 3GPP long term evolution (LTE) standard and its advanced version (LTE-A) [2], due to its good peak-to-average power ratio (PAPR) properties. SC-FDMA can be viewed as a form of orthogonal FDMA (OFDMA) [3] in which an additional discrete fourier transform (DFT) and an inverse DFT (IDFT) are added at the transmitter (TX) and receiver (RX) ends, respectively. A DFT precoder [1] spreads all the symbols across the whole frequency band, forming a virtual SC structure which is known to lead to a reduced PAPR.

This work was supported by the Academy of Finland, Riitta and Jorma J. Takanen Foundation, Finnish Foundation for Technology Promotion, Walter Ahlström Foundation, Ulla Tuominen foundation, KAUTE-foundation and Tauno Tönning foundation. This work was also in part supported by the Japanese government funding program, Grant-in-Aid for Scientific Research (B), No. 23360170.

V. Tervo and A. Tölli are with the Centre for Wireless Communications, University of Oulu, P.O. Box 4500, 90014 University of Oulu, Finland, email: {valtteri.tervo, antti.tolli}@ee.oulu.fi. T. Matsumoto is with the Centre for Wireless Communications, University of Oulu, and Japan Advanced Institute of Science and Technology, 1-1 Asahi-Dai, Nomi, Ishikawa, 923-1292 Japan, email: tadashi.matsumoto@ee.oulu.fi.

It is well known that power allocation in multi-carrier transmission provides significant improvement in terms of total power consumption [4]. In [5], [6], a power allocation technique taking into account the convergence properties of an iterative RX was derived for SC-FDMA showing substantial improvement in terms of reducing the signal-to-noise ratio (SNR) requirements for the desired quality of service (QoS) target. However, the use of frequency domain power allocation leads to an increased value of the PAPR. Motivated by this fact, we have constructed a framework in this paper by which the PAPR can be controlled via frequency domain power allocation.

Reducing the PAPR in any transmission system is always desirable as it allows the use of more efficient and inexpensive power amplifiers (PAs) at the TX. In order to maximize the PA efficiency (PAE), the operating point of the PA should be set as close to the saturation as possible. However, in multi-carrier systems, moving the operation point closer to the saturation increases the probability that the amplified signal components appear in the nonlinear region of the PA. Furthermore, this probability is directly proportional to PAPR. Amplifying the signal components in PAs nonlinear region, introduces out-of-band distortion. Thus, reducing the PAPR induces the following advantages: increased PAE with the same distortion or, decreased distortion with the same PAE.

The problem of PAPR reduction in multi-carrier transmission has been an active research topic for several decades. In the past, the PAPR problem has been addressed in many papers and overview articles, e.g., [7]–[9]. Existing techniques, such as selected mapping (SLM) [10], partial transmit sequences (PTS) [11], [12] and constellation shaping [13]–[15] achieve a reduced PAPR at the expense of a transmit signal power increase, bit error rate (BER) increase, data rate loss, computational complexity increase, etc. The most straightforward solution for PAPR reduction is clipping the amplitude of the OFDM signal. The drawback is that the clipping increases the noise level.

Recent work on reducing the PAPR in SC-FDMA transmission can be found in [16]–[18], where the authors propose different precoding methods for PAPR reduction. In [16], the idea is to use non-diagonal power allocation matrix in OFDMA transmission to distribute the symbols across the subcarriers such that the PAPR is minimized. The idea in the methods presented in [17], [18] is finding the optimal weights for the subcarriers, i.e., power allocation matrix, such that the power variance of the transmitted time domain signal is minimized.

However, the power allocation methods introduced in [16]–[18] solely focus on the PAPR reduction, while the method proposed in this paper considers joint PAPR reduction and sum power minimization. Power allocation methods derived in this paper take also into account a frequency selective channel and an iterative RX.

The main objective in this paper is to improve the PAPR characteristics of a multi-carrier transmission by introducing a novel power allocation method taking into account the properties of an iterative RX and the PAPR of the transmitted signal. The contributions of this paper are summarized as follows: Two approaches for a PAPR aware power allocation in multi-carrier transmission are presented. The first approach optimally restricts the PAPR below a preset threshold value while guaranteeing the preset QoS target. The second approach controls the PAPR statistically by controlling the variance of the power of the transmitted signal. The instantaneous PAPR and the variance are derived for both SC-FDMA and OFDMA. The PAPR and power variance derivations presented in this paper apply in any normalized data modulation technique. The PAPR constraints are applied to the optimization framework presented in [6], where the objective is to minimize the sum power in uplink transmission while guaranteeing the convergence of an iterative equalizer. Two successive convex approximations (SCA) [19] commonly existing in the power control problems are derived for the PAPR constraints. Namely, successive convex approximation via change of variables (SCACOV) [20] and successive convex approximation via geometric programming (SCAGP) [21]. The authors have published the first results on PAPR constrained power allocation in [22], [23] where SCACOV has been derived for instantaneous PAPR constraint and SCAGP has been derived for the power variance constraint. This paper provides a detailed derivation of the constraints and extends the concept to OFDMA. Furthermore, SCAGP is derived for the PAPR constraint and SCACOV is derived for the variance constraint.

The rest of the paper is organized as follows: The system model assumed throughout the paper is presented in Section II. In Section II-A, the TX side of SC-FDMA and OFDMA uplink transmission is described. In Section II-B, iterative equalizers for SC-FDMA and OFDMA are presented. The optimization problem is introduced in Section III. The user specific QoS constraints are presented in Section IV. The PAPR constraints with the SCACOV and SCAGP solutions are presented in Section V and Appendices A-F. The power variance constraints with the SCACOV and SCAGP solutions are presented in Section VI and Appendices G-L. The numerical results are given in Section VII and the conclusions are drawn in Section VIII.

***Nomenclature* –** Following notations are used throughout the paper: Vectors are denoted by lower boldface letters and matrices by uppercase boldface letters. The superscripts $^{\mathrm{H}}$ and $^{\mathrm{T}}$ denote Hermitian and transposition of a complex vector or matrix, respectively. $\mathbb{C}$, $\mathbb{R}$, $\mathbb{B}$ denote the complex, real and binary number fields, respectively. $\mathbf{I}_N$ denotes $N \times N$ identity matrix. The operator avg$\{\cdot\}$ calculates the arithmetic mean of its argument, diag$(\cdot)$ generates diagonal matrix of its arguments, bdiag$\{\cdot\}$ generates the block diagonal matrix from its argument matrices, $\otimes$ denotes the Kronecker product and $\|\cdot\|$ is the Euclidean norm of its complex argument vector. $\mathbb{E}[\cdot]$ is the expectation operator. circ$\{\cdot\}$ constructs a circulant matrix from its argument, in which each column of the matrix is a cyclically shifted version of its successive column. A list of the most relevant symbols used in the paper is shown in Table I.

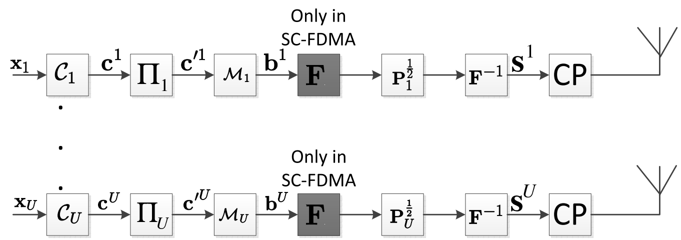

Fig. 1. Block diagram of the TX side of the system model.

II. System Model

In this section, the system model of uplink transmission in a single-cell system with U single-antenna users and a base station with N_R antennas is presented. The channel state information (CSI), including an instantaneous channel impulse response and the second moment of additive thermal noise, is assumed to be perfectly known both at the TX and RX.

A. Transmitter

The TX side of the system model is depicted in Fig. 1. Each user's data stream $\mathbf{x}_u \in \mathbb{B}^{R_c^u N_Q N_F}$, $u = 1, 2, \ldots, U$, is encoded by a forward error correction (FEC) code $\mathcal{C}_u$ with a code rate $R_c^u \leq 1$. The symbol N_Q denotes the number of bits per modulation symbol and N_F is the number of frequency bins in DFT. The encoded bits $\mathbf{c}^u = [c_1^u, c_2^u, \ldots, c_{N_Q N_F}]^{\mathrm{T}} \in \mathbb{B}^{N_Q N_F}$ are bit-interleaved by multiplying $\mathbf{c}^u$ by pseudo-random permutation matrix $\mathbf{\Pi}_u \in \mathbb{B}^{N_Q N_F \times N_Q N_F}$ resulting a bit sequence $\mathbf{c}'^u = \mathbf{\Pi}_u \mathbf{c}^u$. After the interleaving, the sequence $\mathbf{c}'^u$ is mapped with a mapping function $\mathcal{M}_u(\cdot)$ onto a 2^{N_Q}-ary complex symbol $b_l^u \in \mathbb{C}$, $l = 1, 2, \ldots, N_F$, resulting a complex data vector $\mathbf{b}^u = [b_1^u, b_2^u, \ldots, b_{N_F}^u]^{\mathrm{T}} \in \mathbb{C}^{N_F}$. After the modulation, in SC-FDMA each user's data stream is spread across the subchannels by multiplying $\mathbf{b}^u$ by a DFT matrix $\mathbf{F} \in \mathbb{C}^{N_F \times N_F}$, $\forall u = 1, 2, \ldots, U$, where the elements of $\mathbf{F}$ are given by $f_{m,l} = \frac{1}{\sqrt{N_F}} e^{(i2\pi(m-1)(l-1)/N_F)}$, $m, l = 1, 2, \ldots, N_F$. In OFDMA, this spreading process is omitted. Each user's data stream is multiplied with its associated power allocation matrix $\mathbf{P}_u^{\frac{1}{2}}$, where $\mathbf{P}_u = \mathrm{diag}([P_{u,1}, P_{u,2}, \ldots, P_{u,N_F}]^{\mathrm{T}}) \in \mathbb{R}^{N_F \times N_F}$, with $P_{u,l}$ being the power allocated to the lth frequency bin. Finally, before transmission, each user's data stream is transformed into the time domain by the IDFT matrix $\mathbf{F}^{-1}$ resulting in $\mathbf{s}^u = [s_1^u, s_2^u, \ldots, s_{N_F}^u]^{\mathrm{T}}$, $\forall u$. A cyclic prefix is appended to mitigate inter-block interference (IBI) in SC-FDMA and inter-symbol interference (ISI) in OFDMA.

TABLE I
LIST OF SYMBOLS.

$\tilde{b}_l^u$	soft estimate of the u^{th} user's l^{th} symbol	$\boldsymbol{b}^u$	transmitted symbol vector of user u
$\tilde{\boldsymbol{b}}^u$	soft estimate vector of user u	$\hat{\boldsymbol{b}}^u$	time domain estimate vector of user u
$\ddot{\mathbf{b}}^l$	vector for the detected data stream of user u with elements $\lvert\tilde{b}_l^u\rvert^2$	$\boldsymbol{c}^u$	encoded bit vector of user u
$\boldsymbol{c}'^u$	interleaved encoded bit vector of user u	$\mathbf{H}_u$	block circulant channel matrix of user u
N_F	number of bins in discrete Fourier transform	N_L	length of the channel impulse response
N_R	number of receive antennas	N_Q	number of bits per modulation symbol
$\mathbf{P}_u$	diagonal power allocation matrix of user u	$\breve{\mathbf{r}}_u$	combination of the residual and the desired signal associated with user u
$\tilde{\mathbf{r}}_m$	received frequency domain signal vector associated with the m^{th} frequency bin	$\hat{\mathbf{r}}_m$	the output vector of soft cancelation
$\boldsymbol{s}^u$	transmitted symbol vector of user u after IDFT	U	number of users
$\boldsymbol{v}$	vector of noise samples	$\boldsymbol{x}_u$	binary data stream of user u
$\boldsymbol{\gamma}_{u,m}$	channel vector for the m^{th} frequency bin of user u	$\boldsymbol{\Gamma}_u$	frequency domain channel matrix for user u
δ_u	PAPR target for user u	Δ^u	average residual interference of the soft symbol estimates of user u
ζ_u	the effective SINR of user u in SC-FDMA	$\tilde{\zeta}_u$	the effective SINR of user u in OFDMA
$\xi_{u,k}$	auxiliary constant describing the required SINR for given MI target in SC-FDMA	$\tilde{\xi}_{u,k}$	auxiliary constant describing the required SINR for given MI target in OFDMA
σ_v^2	variance of noise	$\tilde{\sigma}_u^2$	power variance target for user u
$\mathring{\sigma}_{u,k}^2$	the variance of the LLRs at the input of the decoder of the u^{th} user at the k^{th} MI index	$\boldsymbol{\Sigma}_{\hat{\mathbf{r}},m}$	interference covariance matrix of the m^{th} frequency bin of user u in SC-FDMA
$\boldsymbol{\Sigma}_{\hat{\mathbf{r}}}$	covariance matrix of the output of the soft cancelation	$\boldsymbol{\omega}_{u,m}$	receive beamforming vector for the m^{th} frequency bin of user u in SC-FDMA
$\tilde{\boldsymbol{\omega}}_{u,m}$	receive beamforming vector for the m^{th} frequency bin of user u in OFDMA	$\breve{\boldsymbol{\Omega}}_u$	filtering matrix of user u

B. Receiver

In this section, frequency domain soft cancelation minimum mean squared error (MMSE) receiver is derived for SC-FDMA and OFDMA.

1) SC-FDMA: For SC-FDMA, the RX presented in [6] is used. After the soft cancelation, the residual and estimated received signal of user u are summed in $\breve{\mathbf{r}}_u \in \mathbb{C}^{N_R N_F}$ as

$$\breve{\mathbf{r}}_u = \sum_{l=1}^{U} \boldsymbol{\Gamma}_l \mathbf{P}_l^{\frac{1}{2}} \mathbf{F}(\mathbf{b}^l - \tilde{\mathbf{b}}^l) + \boldsymbol{\Gamma}_u \mathbf{P}_u^{\frac{1}{2}} \mathbf{F} \tilde{\mathbf{b}}^u + \mathbf{F}_{N_R} \mathbf{v}, \quad (1)$$

where $\tilde{\mathbf{b}}^u \in \mathbb{C}^{N_F}$ is a soft symbol estimate vector composed by $\tilde{\mathbf{b}}^u = [\tilde{b}_1^u, \tilde{b}_2^u, \ldots, \tilde{b}_{N_F}^u]^{\mathrm{T}}$ with $\tilde{b}_n^u$ being the soft symbol estimate of b_n^u given in [6, Eq. (6)]. A matrix $\boldsymbol{\Gamma}_u = \mathrm{bdiag}\{\boldsymbol{\Gamma}_{u,1}, \boldsymbol{\Gamma}_{u,2}, \ldots, \boldsymbol{\Gamma}_{u,N_F}\} \in \mathbb{C}^{N_R N_F \times N_F}$ is the space-frequency channel matrix for user u expressed as $\boldsymbol{\Gamma}_u = \mathbf{F}_{N_R} \mathbf{H}_u \mathbf{F}^{-1}$. The block diagonal DFT matrix $\mathbf{F}_{N_R}$ is expressed as $\mathbf{F}_{N_R} = \mathbf{I}_{N_R} \otimes \mathbf{F} \in \mathbb{C}^{N_R N_F \times N_R N_F}$, and $\boldsymbol{\Gamma}_{u,m} \in \mathbb{C}^{N_R \times N_R}$ is the diagonal channel matrix for the m^{th} frequency bin of the u^{th} user. A matrix $\mathbf{H}_u = [\mathbf{H}_u^1, \mathbf{H}_u^2, \ldots, \mathbf{H}_u^{N_R}]^{\mathrm{T}} \in \mathbb{C}^{N_R N_F \times N_F}$ is the space-time channel matrix for user u and $\mathbf{H}_u^r = \mathrm{circ}\{[h_{u,1}^r, h_{u,2}^r, \ldots, h_{u,N_L}^r, \mathbf{0}_{1 \times N_F - N_L}]^{\mathrm{T}}\} \in \mathbb{C}^{N_F \times N_F}$ is the time domain circulant channel matrix for user u at receive antenna r. The operator circ{} constructs a circulant matrix from its argument vector, N_L denotes the length of the channel impulse response, and $h_{u,l}^r$, $l = 1, 2, \ldots, N_L$, $r = 1, 2, \ldots, N_R$, is the fading factor of multipath channel. A vector $\mathbf{v} \in \mathbb{C}^{N_R N_F}$ in (1) denotes white additive Gaussian noise vector with variance σ_v^2.

The time domain output of the receive filter for the uth user can be written as $\hat{\mathbf{b}}^u = \mathbf{F}^{-1} \breve{\boldsymbol{\Omega}}_u^{\mathrm{H}} \breve{\mathbf{r}}_u$, where $\breve{\boldsymbol{\Omega}}_u = [\breve{\boldsymbol{\Omega}}_u^1, \breve{\boldsymbol{\Omega}}_u^2, \ldots, \breve{\boldsymbol{\Omega}}_u^{N_R}]^{\mathrm{T}} \in \mathbb{C}^{N_R N_F \times N_F}$ is the filtering matrix for the u^{th} user and $\breve{\boldsymbol{\Omega}}_u^r \in \mathbb{C}^{N_F \times N_F}$ is the filtering matrix for the r^{th} receive antenna of the u^{th} user. The effective signal to interference plus noise power ratio (SINR) of the prior symbol estimates for the u^{th} user can be expressed as

$$\zeta_u = \frac{1}{N_F} \sum_{m=1}^{N_F} \frac{P_{u,m} \boldsymbol{\omega}_{u,m}^{\mathrm{H}} \boldsymbol{\gamma}_{u,m} \boldsymbol{\gamma}_{u,m}^{\mathrm{H}} \boldsymbol{\omega}_{u,m}}{\boldsymbol{\omega}_{u,m}^{\mathrm{H}} \boldsymbol{\Sigma}_{\hat{\mathbf{r}},m} \boldsymbol{\omega}_{u,m}}, \quad (2)$$

where $\boldsymbol{\gamma}_{u,m} \in \mathbb{C}^{N_R}$ consists of the diagonal elements of $\boldsymbol{\Gamma}_{u,m}$, i.e., $\boldsymbol{\gamma}_{u,m}$ is the channel vector for the m^{th} frequency bin of user u. The receive beamforming vector for the m^{th} frequency bin of user u is denoted as $\boldsymbol{\omega}_{u,m} = \left[[\breve{\boldsymbol{\Omega}}_u^1]_{[m,m]}, [\breve{\boldsymbol{\Omega}}_u^2]_{[m,m]} \ldots, [\breve{\boldsymbol{\Omega}}_u^{N_R}]_{[m,m]} \right]^{\mathrm{T}} \in \mathbb{C}^{N_R}$, and $\boldsymbol{\Sigma}_{\hat{\mathbf{r}},m} \in \mathbb{C}^{N_R \times N_R}$ is the interference covariance matrix of the m^{th} frequency bin given by

$$\boldsymbol{\Sigma}_{\hat{\mathbf{r}},m} = \sum_{l=1}^{U} P_{l,m} \boldsymbol{\gamma}_{l,m} \boldsymbol{\gamma}_{l,m}^{\mathrm{H}} \Delta^l + \sigma_v^2 \mathbf{I}_{N_R}. \quad (3)$$

The average residual interference of the soft symbol estimates is denoted as $\Delta^l = \mathrm{avg}\{\mathbf{1}_{N_F} - \ddot{\mathbf{b}}^l\}$, where $\ddot{\mathbf{b}}^l = [|\tilde{b}_1^l|^2, |\tilde{b}_2^l|^2, \ldots, |\tilde{b}_{N_F}^l|^2]^{\mathrm{T}} \in \mathbb{C}^{N_F}$. Solving the optimal RX via MMSE criterion yields [24]

$$\breve{\boldsymbol{\Omega}}_u = \frac{1}{\mathrm{avg}\{\ddot{\mathbf{b}}^u\} \zeta_u + 1} \boldsymbol{\Sigma}_{\hat{\mathbf{r}}}^{-1} \boldsymbol{\Gamma}_u \mathbf{P}_u^{\frac{1}{2}}, \quad (4)$$

where $\boldsymbol{\Sigma}_{\hat{\mathbf{r}}} \in \mathbb{C}^{N_R N_F \times N_R N_F}$ is the covariance matrix of the output of the soft cancelation given by

$$\boldsymbol{\Sigma}_{\hat{\mathbf{r}}} = \sum_{l=1}^{U} \boldsymbol{\Gamma}_l \mathbf{P}_l^{\frac{1}{2}} \boldsymbol{\Delta}^l \mathbf{P}_l^{\frac{1}{2}} \boldsymbol{\Gamma}_l^{\mathrm{H}} + \sigma_v^2 \mathbf{I}_{N_R N_F}, \quad (5)$$

and $\boldsymbol{\Delta}^l = \Delta^l \mathbf{I}_{N_F}$.

2) OFDMA: The received signal at the m^{th} subcarrier is

$$\tilde{\mathbf{r}}_m = \sum_{u=1}^{U} \boldsymbol{\gamma}_{u,m} \sqrt{P_{u,m}} b_m^u + \tilde{\mathbf{v}}_m \in \mathbb{C}^{N_R}, \tag{6}$$

where $\tilde{\mathbf{v}}_m \in \mathbb{C}^{N_R}$ denotes white additive Gaussian noise vector with variance σ_v^2. The frequency domain signal after soft cancelation is expressed as

$$\hat{\mathbf{r}}_m = \tilde{\mathbf{r}}_m - \sum_{u=1}^{U} \boldsymbol{\gamma}_{u,m} \sqrt{P_{u,m}} \tilde{b}_m^u. \tag{7}$$

The filtered signal can be expressed as

$$\hat{b}_m^u = \tilde{\boldsymbol{\omega}}_{u,m}^{\mathrm{H}} \breve{\mathbf{r}}_{u,m}, \tag{8}$$

where $\breve{\mathbf{r}}_{u,m} = \hat{\mathbf{r}} + \boldsymbol{\gamma}_{u,m} \sqrt{P_{u,m}} \tilde{b}_m^u$, and $\tilde{\boldsymbol{\omega}}_{u,m} \in \mathbb{C}^{N_R}$ is the receive filter of the u^{th} user at the m^{th} subcarrier which can be found by solving

$$\underset{\tilde{\boldsymbol{\omega}}_{u,m}}{\text{minimize}} \quad \mathbb{E}_{b_m^u, \tilde{\mathbf{v}}_m}[(b_m^u - \hat{b}_m^u)(b_m^u - \hat{b}_m^u)^{\mathrm{H}}]. \tag{9}$$

Substituting the solution of (9) to (8) gives the MMSE estimate of the transmitted symbol as

$$\hat{b}_m^u = \Bigg[(\boldsymbol{\gamma}_{u,m} \boldsymbol{\gamma}_{u,m}^{\mathrm{H}} P_{u,m} + \Big(\sum_{\substack{l=1 \\ l \neq u}}^{U} \boldsymbol{\gamma}_{l,m} \boldsymbol{\gamma}_{l,m}^{\mathrm{H}} P_{l,m} (1 - |\tilde{b}_{l,m}|^2) + \sigma_v^2 \mathbf{I}_{N_R} \Big)^{-1} \boldsymbol{\gamma}_{u,m} \sqrt{P_{u,m}} \Bigg]^{\mathrm{H}} \breve{\mathbf{r}}_{u,m}. \tag{10}$$

Similarly to the case of SC-FDMA, the interference cancelation term $1 - |\tilde{b}_{l,m}|^2$ can be approximated by $\Delta^l = \text{avg}\{\mathbf{1}_{N_F} - \ddot{\mathbf{b}}^l\}$[1] leading to a more compact notation

$$\hat{b}_m^u = [(\boldsymbol{\gamma}_{u,m} \boldsymbol{\gamma}_{u,m}^{\mathrm{H}} P_{u,m} + \Big(\boldsymbol{\Sigma}_{\hat{\mathbf{r}},m}^u \Big)^{-1} \boldsymbol{\gamma}_{u,m} \sqrt{P_{u,m}}]^{\mathrm{H}} \breve{\mathbf{r}}_{u,m}, \tag{11}$$

where

$$\boldsymbol{\Sigma}_{\hat{\mathbf{r}},m}^u = \sum_{\substack{l=1 \\ l \neq u}}^{U} \boldsymbol{\gamma}_{l,m} \boldsymbol{\gamma}_{l,m}^{\mathrm{H}} P_{l,m} \Delta^l + \sigma_v^2 \mathbf{I}_{N_R}. \tag{12}$$

The effective SINR after the MMSE filter is given by

$$\tilde{\zeta}_{u,m} = \frac{P_{u,m} |\boldsymbol{\gamma}_{u,m}^{\mathrm{H}} \tilde{\boldsymbol{\omega}}_{u,m}|^2}{\sum_{\substack{l=1 \\ l \neq u}}^{U} |\boldsymbol{\gamma}_{l,m}^{\mathrm{H}} \tilde{\boldsymbol{\omega}}_{u,m}|^2 P_{l,m} (1 - |\tilde{b}_{l,m}|^2) + \sigma_v^2 \|\tilde{\boldsymbol{\omega}}_{u,m}\|^2}. \tag{13}$$

Thus, the fundamental differences to SC-FMDA are that the received signal decouples such that all the operations can be performed per subcarrier and there is no self interference in the SINR equation unlike in (2).

[1]In fact, Δ^l is an essential approximation in order to use higher order modulations where the power of a symbol is not equal to one. In order to use the approximation Δ^l, the expectation of a symbol power has to be one and the length of a block needs to be large enough.

1: Initialize $\hat{\mathbf{P}} = \hat{\mathbf{P}}^{(0)}$
2: **repeat**
3: Calculate the optimal $\boldsymbol{\Omega}$ from (4).
4: Set $\boldsymbol{\Omega} = \boldsymbol{\Omega}^{(*)}$ and solve problem (14) with variables $\mathbf{P}$. (SCA is employed here)
5: Update $\hat{\mathbf{P}} = \mathbf{P}^{(*)}$
6: **until** Convergence

Fig. 2. Alternating Optimization for SC-FDMA.

III. Optimization problem and solving method

The optimization problem considered in this paper is expressed as

$$\begin{array}{ll} \underset{\mathbf{P}, \breve{\boldsymbol{\Omega}}}{\text{minimize}} & \text{tr}\{\mathbf{P}\} \\ \text{subject to} & z_i(\mathbf{P}, \breve{\boldsymbol{\Omega}}) \leq 0, i = 1, 2, \ldots, N \\ & y_k(\mathbf{P}) \leq 0, k = 1, 2, \ldots, K, \end{array} \tag{14}$$

where $z_i(\mathbf{P}, \breve{\boldsymbol{\Omega}}) \leq 0$, $i = 1, 2, \ldots, N$, is a set of QoS constraints and $y_k(\mathbf{P}) \leq 0$, $k = 1, 2, \ldots, K$, is a set of constraints controlling the PAPR. $\breve{\boldsymbol{\Omega}}$ denotes the set of receive filters of all users and all frequency bins. In this paper, we will derive $y_k(\mathbf{P})$ in the form of

$$y_k(\mathbf{P}) = \sum_{n=1}^{\hat{K}} \rho_n^k P_1^{q_{1n}^k} P_2^{q_{2n}^k} \cdots P_{N_F}^{q_{N_F n}^k}, \quad \rho_n^k, q_{mk}^i \in \mathbb{R}, \tag{15}$$

which can be split as $y_k(\mathbf{P}) = y_k(\mathbf{P})^+ + y_k(\mathbf{P})^-$, where $y_k(\mathbf{P})^+ = \sum_{n=1}^{\hat{K}} \rho_n^{k+} P_1^{q_{1n}^k} P_2^{q_{2n}^k} \cdots P_{N_F}^{q_{N_F n}^k}$, and $y_k(\mathbf{P})^- = \sum_{n=1}^{\hat{K}} \rho_n^{k-} P_1^{q_{1n}^k} P_2^{q_{2n}^k} \cdots P_{N_F}^{q_{N_F n}^k}$, with $\rho_n^{k+} = \max\{0, \rho_n^k\}$ and $\rho_n^{k-} = \min\{0, \rho_n^k\}$. Constraint $y_k(\mathbf{P}) \leq 0$ can be rewritten as

$$y_k(\mathbf{P})^+ \leq -y_k(\mathbf{P})^-, \tag{16}$$

where the functions $y_k(\mathbf{P})^+$ and $-y_k(\mathbf{P})^-$ are referred as *posynomials*. Similarly to [6], posynomials can be transformed into a convex form. However, the function $-y_k(\mathbf{P})^-$ on the RHS of (16) has to be approximated by a concave function to make the overall constraint convex. In this paper, we will show two type of approximations, which are guaranteed to converge towards a local solution.

Note that the PAPR constraints depend only on the power allocation $\mathbf{P}$. Hence, the PAPR constraints derived in this paper can be applied to any SC-FDMA or OFDMA optimization framework. The joint optimization of TX $\mathbf{P}$ and RX $\breve{\boldsymbol{\Omega}}$ can be performed via alternating optimization [6]. The alternating optimization in SC-FDMA is described in Fig. 2, where $\mathbf{P}^{(*)}$ indicates a solution to problem (14) for fixed $\boldsymbol{\Omega}$ and $\boldsymbol{\Omega}^{(*)}$ represents the optimal $\boldsymbol{\Omega}$ for fixed $\mathbf{P}$. The idea is to perform joint optimization by alternating between the TX and RX optimizations, where SCA is employed for TX optimization. Local convex approximations for non-convex constraints needed in SCA are described in forthcoming sections. After solving the approximated convex problem, the solution is used to update the approximation point. Then, the approximated problem is solved again using the new approximation point. This procedure is repeated until convergence.

In the following three sections, we will derive QoS, PAPR and power variance constraints for SC-FDMA and OFDMA. Due to the non-convexity of the constraints, two alternative SCAs are also presented.

IV. QoS constraints

The QoS constraint considered in this paper, is the convergence constraint for iterative RX derived in [6]. Convergence constrained power allocation (CCPA) [6] is a power allocation method for an iterative RX that uses turbo equalization. CCPA takes the convergence properties of the RX into account by utilizing extrinsic information transfer (EXIT) charts. More specifically, the idea is to sample the EXIT chart up to K points and check the convergence condition at each sampled MI value. This approach leads to a problem with several SINR constraints, where each constraint is for a different value of *a priori* information. In this section, the convergence constraint for SC-FDMA and OFDMA is briefly presented.

A. Convergence Constraint for SC-FDMA

The convergence constraint for SC-FDMA can be written as [6, Eq. 20]

$$\frac{1}{N_F}\sum_{m=1}^{N_F}\frac{P_{u,m}|\boldsymbol{\gamma}_{u,m}^{\mathrm{H}}\boldsymbol{\omega}_{u,m}^{k}|^2}{\sum_{l=1}^{U}|\boldsymbol{\gamma}_{l,m}^{\mathrm{H}}\boldsymbol{\omega}_{u,m}^{k}|^2P_{l,m}\Delta_k+\sigma_v^2\|\boldsymbol{\omega}_{u,m}^{k}\|^2}\geq\xi_{u,k},$$
$$u=1,2\ldots,U,\quad k=1,2,\ldots,K, \tag{17}$$

where $\boldsymbol{\omega}_{u,m}^{k}$ is the receive beamformer of the u^{th} user at the m^{th} frequency bin at the k^{th} mutual information (MI) index and Δ_k is the cancelation factor at the k^{th} MI index. Due to the additional DFT spreading at the SC-FDMA TX the symbol sequence is spread across the whole frequency band. Hence, the left hand side (LHS) of (17) is the average SINR taken over all subcarriers. The right hand side (RHS) of (17) is a constant depending on the modulation coding scheme (MCS), the required QoS and the amount of *a priori* information at the k^{th} MI index. (17) is not convex in general and hence, convex approximations presented in [6, Secs. V.B. and V.C.] should be used.

B. Convergence Constraint for OFDMA

Similarly to SC-FDMA, the convergence constraint for OFDMA can be written as

$$\frac{P_{u,m}|\boldsymbol{\gamma}_{u,m}^{\mathrm{H}}\tilde{\boldsymbol{\omega}}_{u,m}^{k}|^2}{\sum_{\substack{l=1\\l\neq u}}^{U}|\boldsymbol{\gamma}_{l,m}^{\mathrm{H}}\tilde{\boldsymbol{\omega}}_{u,m}^{k}|^2P_{l,m}\Delta_k+\sigma_v^2\|\tilde{\boldsymbol{\omega}}_{u,m}^{k}\|^2}\geq\tilde{\xi}_{u,k},$$
$$u=1,2\ldots,U,\;\; m=1,2\ldots,N_F,\;\; k=1,2,\ldots,K, \tag{18}$$

where $\tilde{\xi}_{u,k}=\frac{\mathring{\sigma}_{u,k}^2}{4}$ is a constant depending on the variance of the *a priori* LLRs $\mathring{\sigma}_{u,k}^2$. Constraint (18) is clearly convex with respect to $\mathbf{P}$. In OFDMA, the subcarriers are decoupled for fixed SINR and hence, the constraint (18) is per subcarrier. In practise, one could consider a rate constraint across the subchannels resulting in a varying MCS and thus, bit and power loading algorithms should be considered. However, in this paper we consider fixed SINR target and constant MCS across the subcarriers.

V. Instantaneous PAPR constraint

In this section, we derive instantaneous PAPR constraints for SC-FDMA and OFDMA. In addition, SCACOV and SCAGP are presented for non-convex constraints.

A. PAPR constraint for SC-FDMA

Let s_m^u be the m^{th} output of the transmitted waveform for the u^{th} user after the IDFT. The PAPR constraint in general form is expressed as

$$PAPR(\boldsymbol{s}^u)=\frac{\max_m|s_m^u|^2}{\operatorname{avg}\Big[\mathbb{E}\big\{|s_m^u|^2\big\}\Big]}\leq\delta_u, \tag{19}$$

where $\delta_u\geq1$ is a user specific parameter controlling the PAPR. The max operator can be eliminated by requiring

$$\frac{|s_m^u|^2}{\operatorname{avg}[|s_m^u|^2]}\leq\delta_u,\;\;\forall m=1,2,\ldots,N_F. \tag{20}$$

Assuming $\mathbb{E}\{|b_n^u|\}=1,\ \forall u,n$ and $\mathbb{E}\{b_n^ub_i^{u*}\}=0,\ \forall n\neq i$, where b_n^{u*} denotes the complex conjugate of b_n^u, the average can be calculated as

$$\operatorname{avg}[|s_m^u|^2]=\frac{1}{N_F}\sum_{m=1}^{N_F}\mathbb{E}\Big\{|s_m^u|^2\Big\}=\frac{1}{N_F}\sum_{m=1}^{N_F}P_{u,m}. \tag{21}$$

The assumption $\mathbb{E}\{|b_n^u|\}=1$ can be justified for any modulation scheme with a proper normalization factor.

After a lengthy derivation of $|s_m^u|^2$, shown in Appendix A, the instantaneous PAPR constraint (19) for SC-FDMA can be expressed as

$$\frac{1}{N_F}\sum_{l=1}^{N_F}\Big(\kappa^u+2d_l^u\Big)P_{u,l}+\frac{2}{N_F}\sum_{\substack{n_1,n_2=1\\n_2>n_1}}^{N_F}\hat{\eta}_{n_1n_2m}^{u+}\sqrt{P_{u,n_1}P_{u,n_2}}$$
$$\leq\delta_u\sum_{l=1}^{N_F}P_{u,l}+\frac{2}{N_F}\sum_{\substack{n_1,n_2=1\\n_2>n_1}}^{N_F}(-\hat{\eta}_{n_1n_2m}^{u-})\sqrt{P_{u,n_1}P_{u,n_2}},$$
$$\forall m=1,2,\ldots,N_F,\;\;\forall u=1,2,\ldots,U, \tag{22}$$

where $\kappa^u\in\mathbb{R},\ \forall u,\ d_l^u\in\mathbb{R},\ \forall l,u$, and $\hat{\eta}_{n_1n_2m}^{u+},\hat{\eta}_{n_1n_2m}^{u-}\in\mathbb{R},\ \forall n_1,n_2,m,u$. It can be seen that both sides of (22) are posynomials and hence, the constraint is in the form of (16).

The constraint (22) is a non-convex constraint and many approximations can be applied. For example, the term $\sqrt{P_{u,n_1}P_{u,n_2}}$ existing on both sides of (22) is actually a geometric mean and thus a concave function. While we could directly apply SCA by approximating $\sqrt{P_{u,n_1}P_{u,n_2}}$ on the LHS of (22), we present two SCAs so that the reformulated constraint can be incorporated to the optimization framework introduced in [6, Secs. V.B. and V.C.]. In the following we apply SCACOV and SCAGP for constraint (22).

1) SCACOV: For SCACOV, we reformulate the constraint (22) such that it has a convex and concave part. The concave part can be locally approximated by a linear function and similarly to [6, **Algorithm 2**], a local solution can be found iteratively by updating the approximation point.

1: Set $\hat{\alpha}_{u,m} = \hat{\alpha}_{u,m}^{(0)}, \forall u, m$.
2: **repeat**
3: Solve Eq. (14) with constraints (17) and (23).
4: Update $\hat{\alpha}_{u,m} = \alpha_{u,m}^{(*)}, \forall k$.
5: **until** Convergence.

Fig. 3. Successive convex approximation via change of variables.

Denoting $P_{u,l} = e^{\alpha_{u,l}}$, $u = 1, 2, \ldots, U$, $l = 1, 2, \ldots, N_F$, constraint (22) can be approximated at a point $\hat{\boldsymbol{\alpha}}_u$ as

$$\sum_{l=1}^{N_F} (\kappa^u + 2d_l^u) e^{\alpha_{u,l}} + \frac{2}{N_F} \sum_{\substack{n_1,n_2=1\\ n_2>n_1}}^{N_F} \hat{\eta}_{n_1 n_2 m}^{u+} e^{\frac{1}{2}(\alpha_{u,n_1}+\alpha_{u,n_2})} \leq \hat{T}_m(\boldsymbol{\alpha}_u, \hat{\boldsymbol{\alpha}}_u), \quad u = 1, 2, \ldots, U, m = 1, 2, \ldots, N_F, \tag{23}$$

where $\hat{T}_m(\boldsymbol{\alpha}_u, \hat{\boldsymbol{\alpha}}_u)$ is a local linear approximation of the RHS of (22) after the change of variables (COV). Details are shown in Appendix B.

The SCA algorithm starts by a feasible initialization $\hat{\alpha}_{u,m} = \hat{\alpha}_{u,m}^{(0)}, \forall u, m$. After this, (14) is solved with constraints (17) and (23) and with appropriate change of variables to obtain a solution $\alpha_{u,m}^{(*)}$ which is used as a new point for the linear approximation. The procedure is repeated until convergence. The SCACOV is summarized in Fig. 3. Because the linear approximation $\hat{T}_m(\boldsymbol{\alpha}_u, \hat{\boldsymbol{\alpha}}_u)$ is always below the approximated convex function (RHS of (22)), the points satisfying the approximated constraint (23) always satisfy the original constraint (22). By projecting the optimal solution from the approximated problem to the original convex function (RHS in (38)) the constraint becomes loose and thus, the objective can always be reduced. Hence, the objective value of this type of iterative algorithm converges monotonically towards a local optimum of the original problem.

2) SCAGP: In a standard form of geometric programming (GP) [25] constraint, the LHS is a posynomial and RHS is a monomial. For SCAGP, the constraint needs to be in such a form that it has a posynomial on both sides of the inequality sign. Then, the RHS can be successively approximated by a monomial using [6, Eq. (36)], and a local solution can be found iteratively by updating the parameters in monomial approximation.

Constraint (22) can be approximated $\forall u, m$ using

$$\sum_{l=1}^{N_F} (\kappa^u + 2d_l^u) P_{u,l} + \frac{2}{N_F} \sum_{\substack{n_1,n_2=1\\ n_2>n_1}}^{N_F} \hat{\eta}_{n_1 n_2 m}^{u+} \sqrt{P_{u,n_1} P_{u,n_2}} \leq \hat{\mathcal{A}}_m(\mathbf{P}_u, \boldsymbol{b}^u), \tag{24}$$

where $\hat{\mathcal{A}}_m(\mathbf{P}_u, \boldsymbol{b}^u)$ is a monomial approximation of the RHS of (22). Detailed derivation of SCAGP for PAPR constraint in SC-FDMA is shown in Appendix C.

The LHS is a posynomial and RHS is a monomial and hence, (24) is a valid GP constraint. Similarly to SCACOV, (24) can be used updating the approximation point iteratively. Because the monomial approximation is never above the approximated summation, the same arguments describing the convergence presented for SCACOV apply also in this case. Hence, it is guaranteed that the objective value of the SCA with (24) converges monotonically towards the local optimum of the original problem.

B. PAPR constraint for OFDMA

Similarly to SC-FDMA, the PAPR constraint for OFDMA can be written as

$$\sum_{l=1}^{N_F} |b_l^u|^2 P_{u,l} + \sum_{\substack{n_1,n_2=1\\ n_2>n_1}}^{N_F} \tilde{d}_{mn_2n_1}^{u+} \sqrt{P_{u,n_1} P_{u,n_2}} \leq \delta_u \sum_{l=1}^{N_F} P_{u,l} + \sum_{\substack{n_1,n_2=1\\ n_2>n_1}}^{N_F} (-\tilde{d}_{mn_2n_1}^{u-}) \sqrt{P_{u,n_1} P_{u,n_2}}, \tag{25}$$

where $\tilde{d}_{mn_2n_1}^{u+}, \tilde{d}_{mn_2n_1}^{u-} \in \mathbb{R}$, $\forall u, m, n_1, n_2$. A detailed derivation can be found in Appendix D. The major difference between the OFDMA's PAPR constraint and the SC-FDMA's PAPR constraint presented in (22) is in the factors $\hat{\eta}_{n_1 n_2 m}^{u+}$, $\hat{\eta}_{n_1 n_2 m}^{u-}$, $\tilde{d}_{mn_2n_1}^{u+}$ and $\tilde{d}_{mn_2n_1}^{u-}$. Similarly to Sections V-A1 and V-A2, constraint (25) can be successively approximated as SCACOV or SCAGP. SCACOV and SCAGP derivation can be found in Appendices E and F, respectively.

VI. POWER VARIANCE CONSTRAINT

Another way to reduce the PAPR is to reduce the variance of the power of the transmitted time domain signal [17], [18]. The variance is taken over all possible symbol sequences and therefore, unlike in instantaneous PAPR constraint, the variance constraint does not depend on the transmitted symbol sequence. Note that reducing the power variance leads to statistically decreased PAPR. In this paper, we investigate this relationship of PAPR and power variance by deriving a constraint that restricts the power variance below a desired threshold.

A. Power variance constraint for SC-FDMA

Assuming $\mathbb{E}\{|b_n^u|\} = 1$, $\forall u, n$ and $\mathbb{E}\{b_{n_1}^u b_{n_2}^{u*}\} = 0$, $\forall n_1 \neq n_2$, the power variance constraint can be written as

$$(N_F - 1)(\sum_{l=1}^{N_F} P_{u,l})^2 \leq \sum_{n_1,n_2 \in \mathcal{S}_1}^{N_F} P_{u,n_1} P_{u,n_2} + \sum_{n_1,n_2,n_3,n_4 \in \mathcal{S}_2}^{N_F} \sqrt{P_{u,n_1} P_{u,n_2} P_{u,n_3} P_{u,n_4}} + (\sum_{l=1}^{N_F} P_{u,l})^2 \tilde{\sigma}_u^2 N_F^3, \tag{26}$$

where $\tilde{\sigma}_u^2$ is the preset upper bound of the variance of transmitted power for the u^{th} user. The details, including the definition of the summation sets $\mathcal{S}_1$ and $\mathcal{S}_2$, can be found in Appendix G. Both sides of (26) are posynomials. Thus, SCA is needed for the RHS. Both, SCACOV and SCAGP are applied for approximating (26) in Appendices H and I, respectively.

B. Power variance constraint for OFDMA

In the case of OFDMA, the variance constraint is written as

$$\frac{2}{N_F^2} \sum_{\substack{n_1,n_2=1 \\ n_2>n_1}}^{N_F} P_{u,n_2} P_{u,n_1} \leq \tilde{\sigma}_u^2 \left(\sum_{m=1}^{N_F} P_{u,m} \right)^2 . \quad (27)$$

The details are shown in Appendix J. Again, both sides of (27) are posynomials. Thus, SCA is needed for the RHS of (27). Both, SCACOV and SCAGP are applied for approximating (27) in Appendices K and L, respectively.

VII. Numerical Results

In this section, the results obtained in the simulations are presented.

A. Simulation setup

The results are obtained with the following parameters: $N_F = 8$, quadrature phase-shift keying (QPSK) ($N_Q = 2$) and 16-ary quadrature amplitude modulation (16QAM) ($N_Q = 4$) with Gray mapping, and systematic repeat accumulate (RA) code [26] with a code rate of 1/3 and eight internal iterations. Uniform diagonal sampling [6] is used for EXIT sampling in the QoS constraint, and the number of samples is $K = 5$. The SNR per user and per RX antenna averaged over frequency bins is defined by SNR= $\mathrm{tr}\{\mathbf{P}\}/(UN_RN_F\sigma_v^2)$. We consider two different channel conditions, namely, a static 5-path channel, where path gains were generated randomly, and a quasi-static Rayleigh fading 5-path average equal gain channel. The stopping criterion of the optimization algorithms is that the change in the objective function becomes less than or equal to a small specific value between two successive iterations. In simulations, the stopping threshold value was set at 0.05 for TX-RX alternations and 0.01 for SCAs.

Let $\hat{I}_u^{\mathrm{E}}$ and $\mathring{I}_u^{\mathrm{E}}$ denote the MI at the output of the equalizer of the u^{th} user and at the output of the decoder of the u^{th} user, respectively. The QoS target used in the simulations is the MI target after the turbo iterations in the RX denoted as $\mathring{I}_u^{\mathrm{E,target}}$ and $\hat{I}_1^{\mathrm{E,target}}$. MI point can be converted to bit error probability (BEP) by using [27, Eq. (31)].

The PAPR cannot be considered as the only performance metric since there is often a tradeoff between the PAPR and the average power, i.e., a decrease in PAPR may lead to an increase of the average power and vice versa. The peak power of the transmission is defined as $P_{\max}(dB) = P_{\mathrm{avg}}(dB) + PAPR(dB)$, where $P_{\mathrm{avg}} = SNR \times N_R \times \sigma_v^2$ denotes the average power of user u. If the peak power can be reduced, the average power can be increased and thus, we can use the metric $SNR(dB) + PAPR(dB)$ to compare the algorithms in terms of the range of the transmission.

B. Initialization

To employ the SCAs presented in this paper, it is necessary to find a feasible starting point for the iterative algorithm. In the case of SC-FDMA, it can be found by setting the power to be equal for all subcarriers. The power level has to be high enough to satisfy the QoS constraints and it can be found by using a bisection algorithm [25]. In equal allocation, the PAPR is 0 dB and 2.55 dB for QPSK and 16QAM, respectively, which are the modulation schemes considered in the simulations. As long as the target PAPR is above this value, the result obtained by equal allocation satisfies the PAPR constraint for SC-FDMA.

1: Calculate the ZF matrix for the frequency domain channel.
2: Find the power allocation satisfying QoS constraint.
3: **repeat**
4: Set $P_{u,n} = P_{u,n} + \epsilon$, for all u, for some $n \in \{1, 2, \ldots, N_F\}$, and $\epsilon > 0$.
5: Calculate PAPR for all the users PAPR_u.
6: **until** PAPR$\leq \delta_u$

Fig. 4. Initialization of the optimization algorithm in OFDMA.

In the case of OFDMA, a feasible starting point for the iterative algorithm can be found, for example, with the help of spatial zero forcing (ZF) [4] RX. It is straightforward to show that, for OFDMA, $\frac{\max_m |s_m^u|^2}{\mathrm{avg}[|s_m^u|^2]} \rightarrow 1$ when $P_{u,n} \rightarrow \infty$ for some n. Increasing $P_{u,n}$ does not violate the SINR constraint because ZF RX removes all the interference. The feasible initialization method is summarized in Fig. 4. Step 2 can be performed by allocating the same power for all the subcarriers. The power level can be found by using a bisection algorithm [25]. This initialization method presented above applies also with appropriate modifications for a power variance-constrained problem. Numerical results revealed that in this particular case the optimization is not highly sensitive to initializations. It is worthwhile to notice that in all results presented in this paper, SCACOV and SCAGP converge towards the same objective value.

C. PAPR constraint

To demonstrate the operational principle of the PAPR constraint, EXIT simulations were carried out in a static channel for a fixed symbol sequence. The EXIT curve of the decoder is obtained by using 200 blocks for each *a priori* value, with the size of a block being 6000 bits. The EXIT chart of the turbo equalizer when precoding with instantaneous PAPR constraint is presented in Fig. 5. SC-FDMA and OFDMA denote the schemes without the PAPR constraint, i.e., with the QoS constraint only. The SC-FDMA result is obtained via SCAGP approximation. Clipping denotes the case where the signal is clipped when the power exceeds the peak value calculated from the PAPR threshold. The minimum gap between the EXIT curves of the equalizer and the decoder of user u can be controlled by changing the parameter ${\epsilon_u}^2$.

It can be also seen from Fig. 5 that, with SC-FDMA, the minimum gap between the EXIT curves can be suppressed down to ϵ_u according to the convergence constraint. For OFDMA, the gap is larger than ϵ_u, which results in significantly larger SNR requirements compared to SC-FDMA. This can be seen in Table II, where the corresponding SNR and

[2] The reader is guided to [6] for more detailed information on CCPA.

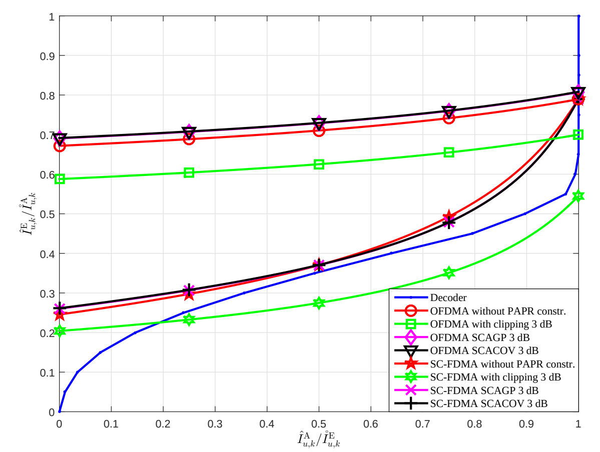

Fig. 5. EXIT chart for $\delta_u = 3$ dB. $U = 2$, $N_R = 2$, $N_Q = 2$, $\hat{I}_u^{\mathrm{E,target}} = 0.7892$, $u = 1, 2$, $\mathring{I}_u^{\mathrm{E,target}} = 0.9998$, $u = 1, 2$, $\epsilon_u = 0.02$, $u = 1, 2$, $\mathbf{b}^1 = 1/\sqrt{2}[-1-i, -1-i, -1-i, 1+i, -1-i, 1+i, 1-i, 1+i]^{\mathrm{T}}$, $\mathbf{b}^2 = 1/\sqrt{2}[-1+i, -1+i, 1-i, -1+i, -1+i, -1-i, -1+i, -1+i]^{\mathrm{T}}$.

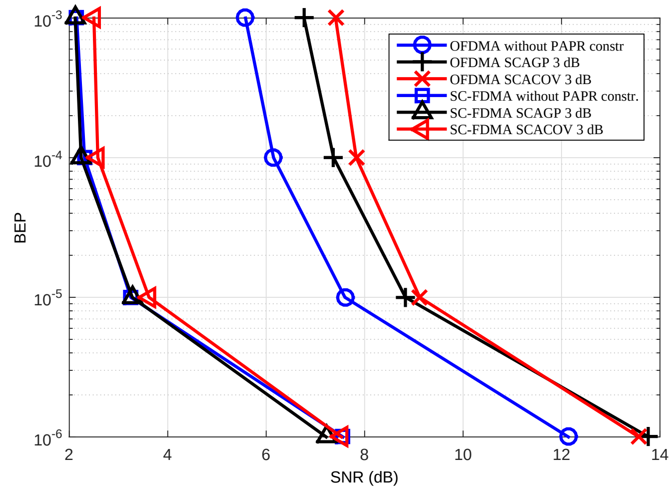

Fig. 6. BEP comparison with $\delta_u = 3$ dB. $U = 2$, $N_R = 2$, $N_Q = 2$, $\epsilon_u = 0.1$, $u = 1, 2$.

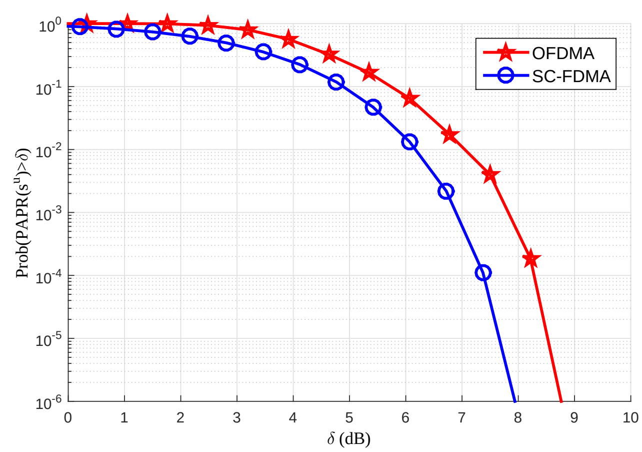

Fig. 7. CCDFs for SC-FDMA and OFDMA with BEP target 10^{-5}. $U = 2$, $N_R = 2$, $N_Q = 2$, $\hat{I}_u^{\mathrm{E,target}} = 0.7892$, $u = 1, 2$, $\mathring{I}_u^{\mathrm{E,target}} = 0.9998$, $u = 1, 2$, $\epsilon_u = 0.1$, $u = 1, 2$.

PAPR are listed together with the summation of SNR and PAPR for each algorithm used. The larger SNR requirement of OFDMA compared to SC-FDMA is due to the difference in convergence constraints. In the case of OFDMA, the SINR requirement is the same for all subcarriers, unlike in SC-FDMA where the average of SINRs over the subcarriers is used. On the other hand, there is no intra-user interference in OFDMA, unlike in SC-FDMA for which the starting point in the EXIT chart is interference-limited. Hence, the target point in the case of OFDMA can be achieved even with linear RX by simply increasing the power in all the subcarriers. Clipping reduces the SNR but convergence to the desired MI point is not guaranteed. In the case of SC-FDMA with clipping, the EXIT curves intersect at MI point $(\mathring{I}_u^{\mathrm{E}}, \hat{I}_u^{\mathrm{E}}) = (0.1936, 0.2254)$, which corresponds to BEP value 0.2053.

It can be seen from Table II that the PAPR threshold used in Fig. 5 is not exceeded with the PAPR constraint. The sum of SNR and PAPR describes the actual power gain achieved by the proposed algorithms, which helps to improving the QoS for cell edge users. It can be seen that in the case of OFDMA the improvement when using the PAPR constraint is 9.31 dB $-$ 8.44 dB $=$ 0.87 dB. In the case of SC-FDMA, the improvement is 3.16 dB and 3.17 dB for SCAGP and SCACOV, respectively.

In Fig. 6, the required SNR versus BEP is presented, where the results are obtained by averaging over 200 channel realizations. Four different BEP target values are considered for $u = 1, 2$, namely 10^{-3}, 10^{-4}, 10^{-5} and 10^{-6}. It can be seen that for SC-FDMA, the required SNR is roughly the same with and without the PAPR constraint, i.e., the PAPR can be suppressed to 3 dB without a significant increase in transmit power. For OFDMA, the required SNR is increased by 1.19-1.83 dB, depending on the BEP target and algorithm used.

Complementary cumulative distribution functions (CCDF) Prob$(PAPR > \delta)$ for SC-FDMA and OFDMA without PAPR constraints and with a BEP target of 10^{-5} are plotted in Fig. 7. CCDFs are calculated such that 10^5 randomly generated symbol sequences of length N_F for each user are sent over 200 channel realizations. Obviously, for the algorithms with PAPR constraint, the CCDF is 0 when the PAPR is larger than the PAPR threshold. For a CCDF value of 10^{-5}, the corresponding PAPRs are 7.66 dB and 8.52 dB for SC-FDMA and OFDMA, respectively. From Figs. 6 and 7, we can calculate the SNR+PAPR gains for SC-FDMA to be 4.63 dB and 4.29 dB for SCAGP and SCACOV, respectively. Similarly for OFDMA, the gains are 4.29 dB and 4.00 dB, respectively.

D. Power variance constraint

CCDFs for the OFDMA scheme when precoding with a variance constraint is shown in Fig. 8. It can be seen that the PAPR can be significantly reduced by decreasing the variance. In fact, the PAPR approaches the theoretical limit,, i.e., 2.55 dB for 16 QAM when the variance target approaches zero. However, because the per-subcarrier SINR constraint is

TABLE II
SNR AND PAPR COMPARISON IN A STATIC CHANNEL

Algorithm	SNR (dB)	PAPR (dB)	SNR + PAPR (dB)
OFDMA	4.97	4.34	9.31
OFDMA with clipping	4.37	3.00	7.37
OFDMA SCAGP	5.44	3.00	8.44
OFDMA SCACOV	5.46	2.98	8.44
SC-FDMA	1.38	6.22	7.60
SC-FDMA with clipping	0.49	3.00	3.49
SC-FDMA SCAGP	1.44	3.00	4.44
SC-FDMA SCACOV	1.44	2.99	4.43

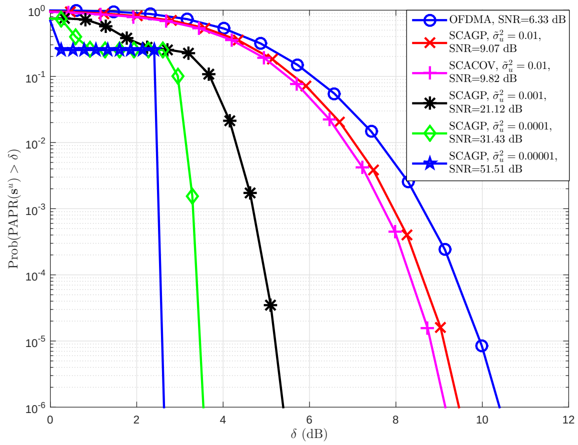

Fig. 8. CCDFs for OFDMA with variance constraint. BEP target=10^{-5}, $U = 4$, $N_R = 4$, $N_Q = 4$, $\hat{I}_u^{\text{E,target}} = 0.7892$, $\forall u$, $\mathring{I}_u^{\text{E,target}} = 0.9998$, $\forall u$, $\epsilon_u = 0.1$, $\forall u$.

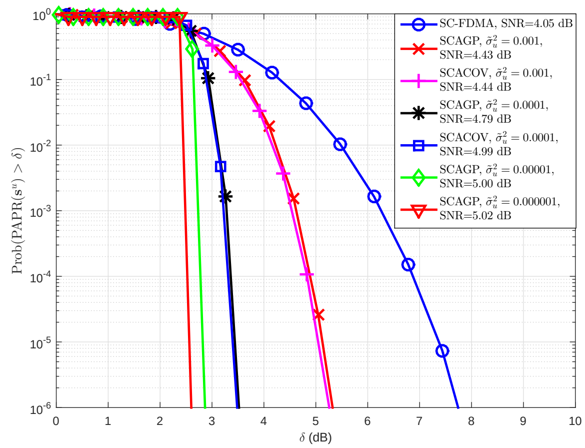

Fig. 9. CCDFs for SC-FDMA with variance constraint. BEP target=10^{-5}, $U = 4$, $N_R = 4$, $N_Q = 4$, $\hat{I}_u^{\text{E,target}} = 0.7892$, $\forall u$, $\mathring{I}_u^{\text{E,target}} = 0.9998$, $\forall u$, $\epsilon_u = 0.1$, $\forall u$.

used as a QoS constraint, the SNR increase is high compared to the PAPR reduction.

CCDFs for the SC-FDMA scheme when precoding with a variance constraint are shown in Fig. 9. It can be seen that the PAPR can be significantly reduced with a minor increase in SNR by decreasing the power variance. Similarly to the OFDMA case, the PAPR approaches the theoretical limit when the variance target approaches zero.

VIII. CONCLUSIONS

In this paper, we have formulated PAPR constrained power allocation problem for multicarrier transmission with iterative MMSE multiuser multiantenna RX. We derived an analytical expression of PAPR as a function of transmit power allocation for SC-FDMA and OFDMA. The derived PAPR constraints are applicable for any normalized data modulation format. In addition, a statistical approach considering the transmission power variance constrained power allocation was derived. Two different successive convex approximations were derived for all the proposed constraints. Numerical results indicate that instead of amplitude clipping, the PAPR constraint is of crucial importance to guarantee the convergence of an iterative equalizer. It was also observed that the proposed techniques can significantly improve the efficiency of the transmission of power limited users. Hence, the constraints derived in this paper are especially beneficial for the users on the cell edge because the coverage area of the cell can be increased for a given QoS target.

The PAPR and the variance constraints depend only on the local information, i.e., the power allocation and the transmitted symbol sequence in the case of instantaneous PAPR constraint, and the power allocation only in the case of the power variance constraint. If the QoS constraint requires centralized processing, the intuition is that the power variance constraint is a better alternative because it does not require information about the transmitted symbol sequence. However, if the QoS constraint can be handled by using the local information, instantaneous PAPR constraint can be used because the information about the symbol sequence is available.

Appendix A
The instantaneous power of the transmitted signal in SC-FDMA

The power of the transmitted waveform of user u at time instant m is calculated as

$$
\begin{aligned}
|s_m^u|^2 &= |\sum_{n=1}^{N_F} g_{m,n}^u b_n^u|^2 \\
&= \frac{1}{N_F^2}\Bigg(\sum_{n=1}^{N_F}\Big(b_n^u b_n^{u*}\Big(\sum_{l=1}^{N_F}\sqrt{P_{u,l}}a_{lnm}\Big)^2\Big) \\
&+ \sum_{\substack{n_1,n_2=1\\ n_1\neq n_2}}^{N_F}\Big(b_{n_1}^u b_{n_2}^{u*}\Big(\sum_{l=1}^{N_F}\sqrt{P_{u,l}}a_{ln_1m}\Big)\Big(\sum_{l=1}^{N_F}\sqrt{P_{u,l}}a_{ln_2m}\Big)\Big)\Bigg) \\
&= \frac{1}{N_F^2}\Bigg(\sum_{n=1}^{N_F}|b_n^u|^2\sum_{l=1}^{N_F}P_{u,l}+ \\
&\sum_{n=1}^{N_F}|b_n^u|^2\sum_{\substack{n_1,n_2=1\\ n_1\neq n_2}}^{N_F}\sqrt{P_{u,n_1}P_{u,n_2}}a_{nn_1n_2}a_{mn_1n_2}^* \\
&+ \sum_{\substack{n_1,n_2=1\\ n_1\neq n_2}}^{N_F} b_{n_1}^u b_{n_2}^{u*}\sum_{l=1}^{N_F}P_{u,l}a_{ln_1q} \\
&+ \sum_{\substack{n_1,n_2=1\\ n_1\neq n_2}}^{N_F} b_{n_1}^u b_{n_2}^{u*}\sum_{\substack{n_1',n_2'=1\\ n_1'\neq n_2'}}^{N_F}\sqrt{P_{u,n_1'}P_{u,n_2'}}a_{n_1'n_1m}a_{n_2'n_2m}^*\Bigg),
\end{aligned} \tag{28}
$$

where $g_{m,n}^u = \frac{1}{N_F}\sum_{q=1}^{N_F}\sqrt{P_{u,q}}a_{qmn}$ and $a_{qmn} = e^{\frac{j2\pi(q-1)(m-n)}{N_F}}$. The second term of (28) can be rewritten as

$$
\sum_{n=1}^{N_F}|b_n^u|^2\sum_{\substack{n_1,n_2=1\\ n_1\neq n_2}}^{N_F}\sqrt{P_{u,n_1}P_{u,n_2}}a_{nn_1n_2}a_{mn_1n_2}^* = \sum_{\substack{n_1,n_2=1\\ n_1\neq n_2}}^{N_F}\beta_{mn_1n_2}^u\sqrt{P_{u,n_1}P_{u,n_2}}, \tag{29}
$$

where

$$
\beta_{mn_1n_2}^u = \sum_{n=1}^{N_F}|b_n^u|^2\Big(\mathcal{R}[a_{nn_1n_2}]\mathcal{R}[a_{mn_1n_2}]+ \mathcal{I}[a_{mn_1n_2}]\mathcal{I}[a_{nn_1n_2}]\Big). \tag{30}
$$

Operators $\mathcal{R}$ and $\mathcal{I}$ in (30) take the real and imaginary part of a complex argument, respectively.

The third term of (28) can rewritten as

$$
\frac{1}{N_F^2}\sum_{\substack{n_1,n_2=1\\ n_1\neq n_2}}^{N_F} b_{n_1}^u b_{n_2}^{u*}\sum_{l=1}^{N_F}P_{u,l}a_{ln_1n_2} = \frac{1}{N_F^2}\sum_{l=1}^{N_F}P_{u,l}2d_l^u, \tag{31}
$$

where

$$
d_l^u = \sum_{\substack{n_2,n_1=1\\ n_1>n_2}}^{N_F}\Big(\mathcal{R}[a_{ln_1n_2}](\mathcal{R}[b_{n_1}^u]\mathcal{R}[b_{n_2}^u]+\mathcal{I}[b_{n_1}^u]\mathcal{I}[b_{n_2}^u])+ \mathcal{I}[a_{ln_1n_2}](\mathcal{R}[b_{n_1}^u]\mathcal{I}[b_{n_2}^u]-\mathcal{I}[b_{n_1}^u]\mathcal{R}[b_{n_2}^u])\Big). \tag{32}
$$

Denoting

$$
\begin{aligned}
\eta_{n_1n_2m}^u = \sum_{\substack{n_4,n_3=1\\ n_3>n_4}}^{N_F}\Big(&(\mathcal{R}[b_{n_3}^u]\mathcal{R}[b_{n_4}^u]+\mathcal{I}[b_{n_3}^u]\mathcal{I}[b_{n_4}^u]) \\
&(\mathcal{R}[a_{n_1n_3m}a_{n_2n_4m}^*]+\mathcal{R}[a_{n_1n_4m}a_{n_2n_3m}^*])- \\
&(\mathcal{I}[b_{n_3}^u]\mathcal{R}[b_{n_4}^u]-\mathcal{R}[b_{n_3}^u]\mathcal{I}[b_{n_4}^u])(\mathcal{I}[a_{n_1n_3m}a_{n_2n_4m}^*] \\
&-\mathcal{I}[a_{n_1n_4m}a_{n_2n_3m}^*])\Big),
\end{aligned} \tag{33}
$$

the last term of (28) can be expressed as

$$
\frac{1}{N_F^2}\sum_{\substack{n_1,n_2=1\\ n_1\neq n_2}}^{N_F} b_{n_1}^u b_{n_2}^{u*}\sum_{\substack{n_1',n_2'=1\\ n_1'\neq n_2'}}^{N_F}\sqrt{P_{u,n_1'}P_{u,n_2'}}a_{n_1'n_1m}a_{n_2'n_2m}^* = 2\sum_{\substack{n_1,n_2=1\\ n_2>n_1}}^{N_F}\eta_{n_1n_2m}^u\sqrt{P_{u,n_1}P_{u,n_2}}. \tag{34}
$$

Substituting (29), (31) and (34) to (28), the signal power is expressed as

$$
|s_m^u|^2 = \frac{1}{N_F^2}\sum_{l=1}^{N_F}\Big(\kappa^u+2d_l^u\Big)P_{u,l}+ \frac{2}{N_F^2}\sum_{\substack{n_1,n_2=1\\ n_2>n_1}}^{N_F}\Big(\beta_{mn_1n_2}^u+\eta_{n_1n_2m}^u\Big)\sqrt{P_{u,n_1}P_{u,n_2}}, \tag{35}
$$

where $\kappa^u = \sum_{n=1}^{N_F}|b_n^u|^2$.

The term $\kappa^u+2d_l^u$ can be rewritten as

$$
\kappa^u+2d_l^u = \Big(\sum_{n=1}^{N_F}b_n^u a_{ln1}\Big)\Big(\sum_{n=1}^{N_F}b_n^u a_{ln1}\Big)^* \geq 0. \tag{36}
$$

However, the factor $\beta_{mn_1n_2}^u+\eta_{n_1n_2m}^u$ can be negative, depending on the symbol sequence and the power allocation. Let $\hat{\eta}_{n_1n_2m}^{u+} = \max\{0,\beta_{mn_1n_2}^u+\eta_{n_1n_2m}^u\}$ and $\hat{\eta}_{n_1n_2m}^{u-} = \min\{\beta_{mn_1n_2}^u+\eta_{n_1n_2m}^u,0\}$. In such a case, the instantaneous PAPR constraint can be written as

$$
\begin{aligned}
&\frac{1}{N_F}\sum_{l=1}^{N_F}\Big(\kappa^u+2d_l^u\Big)P_{u,l}+\frac{2}{N_F}\sum_{\substack{n_1,n_2=1\\ n_2>n_1}}^{N_F}\hat{\eta}_{n_1n_2m}^{u+}\sqrt{P_{u,n_1}P_{u,n_2}} \\
&\leq \delta_u\sum_{l=1}^{N_F}P_{u,l}+\frac{2}{N_F}\sum_{\substack{n_1,n_2=1\\ n_2>n_1}}^{N_F}(-\hat{\eta}_{n_1n_2m}^{u-})\sqrt{P_{u,n_1}P_{u,n_2}}, \\
&\forall m=1,2,\ldots,N_F,\ \ \forall u=1,2,\ldots,U,
\end{aligned} \tag{37}
$$

where all the terms in each summation are non-negative. It should be noted that the number of summation terms in (35) increases in the order of $N_F^4-N_F^2(1+2\sum_{n=1}^{N_F-1}n)+N_F+(\sum_{n=1}^{N_F-1}n)^2$, where the negative term is due to the inequality sign in summation limits in (35).

APPENDIX B
SCACOV FOR PAPR CONSTRAINT IN SC-FDMA

Denoting $P_{u,l} = e^{\alpha_{u,l}}$, $u = 1, 2, \ldots, U$, $l = 1, 2, \ldots, N_F$, constraint (22) becomes

$$\begin{aligned}\frac{1}{N_F}\sum_{l=1}^{N_F}(\kappa^u + 2d_l^u)e^{\alpha_{u,l}} + \frac{2}{N_F}\sum_{\substack{n_1,n_2=1\\ n_2>n_1}}^{N_F}\hat{\eta}_{n_1n_2m}^{u+}e^{\frac{1}{2}(\alpha_{u,n_1}+\alpha_{u,n_2})}\\ \le \delta_u\sum_{l=1}^{N_F}e^{\alpha_{u,l}} + \frac{2}{N_F}\sum_{\substack{n_1,n_2=1\\ n_2>n_1}}^{N_F}(-\hat{\eta}_{n_1n_2m}^{u-})e^{\frac{1}{2}(\alpha_{u,n_1}+\alpha_{u,n_2})}.\end{aligned} \tag{38}$$

The summation of exponentials is convex, and hence both sides of (38) are convex functions.

Let

$$\begin{aligned}T_m(\boldsymbol{\alpha}_u) =&\delta_u\sum_{l=1}^{N_F}e^{\alpha_{u,l}}+\\ &\frac{2}{N_F}\sum_{\substack{n_1,n_2=1\\ n_2>n_1}}^{N_F}(-\hat{\eta}_{n_1n_2m}^{u-})e^{\frac{1}{2}(\alpha_{u,n_1}+\alpha_{u,n_2})},\end{aligned}$$

where $\boldsymbol{\alpha}_u = [\alpha_{u,1}, \alpha_{u,2}, \ldots, \alpha_{u,N_F}]^{\mathrm{T}}$. The best concave approximation of $T_m(\boldsymbol{\alpha}_u)$ at a point $\hat{\boldsymbol{\alpha}}_u$ is given by

$$\hat{T}_m(\boldsymbol{\alpha}_u, \hat{\boldsymbol{\alpha}}_u) = T_m(\hat{\boldsymbol{\alpha}}_u)+\sum_{k=1}^{N_F}\frac{\partial T_m}{\partial \alpha_{u,k}}(\hat{\boldsymbol{\alpha}}_u)(\alpha_{u,k}-\hat{\alpha}_{u,k}). \tag{39}$$

The partial derivative $\frac{\partial T_m}{\partial \alpha_{u,k}}$ is derived as

$$\begin{aligned}\frac{\partial T_m}{\partial \alpha_{u,k}} = \quad & \delta_u e^{\alpha_{u,k}} + \tfrac{1}{N_F}\textstyle\sum_{n=k+1}^{N_F}(-\hat{\eta}_{knm}^{u-})e^{\frac{1}{2}(\alpha_{u,k}+\alpha_{u,n})}\\ &+\tfrac{1}{N_F}\textstyle\sum_{n=1}^{k-1}(-\hat{\eta}_{nkm}^{u-})e^{\frac{1}{2}(\alpha_{u,n}+\alpha_{u,k})}.\end{aligned} \tag{40}$$

The best convex approximation of (38) at a point $\hat{\boldsymbol{\alpha}}_u$ is written as

$$\begin{aligned}\sum_{l=1}^{N_F}(\kappa^u + 2d_l^u)e^{\alpha_{u,l}} + \frac{2}{N_F}\sum_{\substack{n_1,n_2=1\\ n_2>n_1}}^{N_F}\hat{\eta}_{n_1n_2m}^{u+}e^{\frac{1}{2}(\alpha_{u,n_1}+\alpha_{u,n_2})}\\ \le \hat{T}_m(\boldsymbol{\alpha}_u, \hat{\boldsymbol{\alpha}}_u),\quad u = 1, 2, \ldots, U, m = 1, 2, \ldots, N_F.\end{aligned} \tag{41}$$

APPENDIX C
SCAGP FOR PAPR CONSTRAINT IN SC-FDMA

Let

$$\begin{aligned}\mathcal{A}_m(\mathbf{P}_u) = \delta_u\sum_{l=1}^{N_F}P_{u,l}+\\ \frac{2}{N_F}\sum_{\substack{n_1,n_2=1\\ n_2>n_1}}^{N_F}(-\hat{\eta}_{n_1n_2m}^{u-})\sqrt{P_{u,n_1}P_{u,n_2}}.\end{aligned} \tag{42}$$

Applying [6, Eq. (36)][3] to $\mathcal{A}_m(\mathbf{P}_u)$ yields a lower bound (43), where

$$\begin{aligned}\theta_{ul}^{(1)} &= \frac{P_{u,l}}{\sum_{l'=1}^{N_F}P_{u,l'}},\\ \theta_{n_1n_2mu}^{(2)} &= \frac{-\hat{\eta}_{n_1n_2m}^{u-}\sqrt{P_{u,n_1}P_{u,n_2}}}{\sum_{\substack{n_1',n_2'=1\\ n_2'>n_1'}}^{N_F}-\hat{\eta}_{n_1'n_2'm}^{u-}\sqrt{P_{u,n_1'}P_{u,n_2'}}},\end{aligned} \tag{44}$$

and $\tau_{um}^{(1)}$ and $\tau_{um}^{(2)}$ are given in (45). Hence, constraint (22) can be approximated $\forall u, m$ using (46).

APPENDIX D
PAPR CONSTRAINT FOR OFDMA

Similarly to SC-FDMA, the average power in the case of OFDMA is

$$\mathrm{avg}[|s_m^u|^2] = \frac{1}{N_F}\sum_{l=1}^{N_F}P_{u,l}, \tag{47}$$

i.e., the same as in the case of SC-FDMA.

The power of the m^{th} transmitted waveform can be calculated as

$$|s_m^u|^2 = \frac{1}{N_F}\sum_{l=1}^{N_F}|b_l^u|^2P_{u,l} + \frac{1}{N_F}\sum_{\substack{n_1,n_2=1\\ n_2>n_1}}^{N_F}\tilde{d}_{mn_2n_1}^u\sqrt{P_{u,n_1}P_{u,n_2}}, \tag{48}$$

where

$$\begin{aligned}\tilde{d}_{mn_2n_1}^u = 2\Bigg(&\mathcal{R}[a_{mn_2n_1}]\Big(\mathcal{R}[b_{n_2}^u]\mathcal{R}[b_{n_1}^u] + \mathcal{I}[b_{n_2}^u]\mathcal{I}[b_{n_1}^u]\Big)\\ &-\mathcal{I}[a_{mn_2n_1}]\Big(\mathcal{R}[b_{n_2}^u]\mathcal{I}[b_{n_1}^u] - \mathcal{I}[b_{n_2}^u]\mathcal{R}[b_{n_1}^u]\Big)\Bigg).\end{aligned} \tag{49}$$

The number of summation terms in (48) increases in the order or $N_F^2 - \sum_{n=1}^{N_F-1}n$. The PAPR constraint for OFDMA can be written as

$$\begin{aligned}\sum_{l=1}^{N_F}|b_l^u|^2P_{u,l} + \sum_{\substack{n_1,n_2=1\\ n_2>n_1}}^{N_F}\tilde{d}_{mn_2n_1}^{u+}\sqrt{P_{u,n_1}P_{u,n_2}}\\ \le \delta_u\sum_{l=1}^{N_F}P_{u,l} + \sum_{\substack{n_1,n_2=1\\ n_2>n_1}}^{N_F}(-\tilde{d}_{mn_2n_1}^{u-})\sqrt{P_{u,n_1}P_{u,n_2}},\end{aligned} \tag{50}$$

where $\tilde{d}_{mn_2n_1}^{u+} = \max\{0, \tilde{d}_{mn_2n_1}^u\}$ and $\tilde{d}_{mn_2n_1}^{u-} = \min\{\tilde{d}_{mn_2n_1}^u, 0\}$.

APPENDIX E
SCACOV FOR PAPR CONSTRAINT IN OFDMA

Changing the variables as $P_{u,m} = e^{\alpha_{u,m}}$, $\forall u, m$, the approximation of (25) is written as

$$\sum_{l=1}^{N_F}|b_l^u|^2e^{\alpha_{u,l}} + \sum_{\substack{n_1,n_2=1\\ n_2>n_1}}^{N_F}\tilde{d}_{mn_2n_1}^{u+}e^{\frac{1}{2}(\alpha_{u,n_1}+\alpha_{u,n_2})} \le \hat{T}_m(\boldsymbol{\alpha}_u, \hat{\boldsymbol{\alpha}}_u), \tag{51}$$

[3]This bound is derived using the inequality of weighted arithmetic mean and weighted geometric mean.

$$\mathcal{A}_m(\mathbf{P}_u) \geq \left(\frac{\delta_u \prod_{l=1}^{N_F}\left(\frac{P_{u,l}}{\theta_{ul}^{(1)}}\right)^{\theta_{ul}^{(1)}}}{\tau_{um}^{(1)}}\right)^{\tau_{um}^{(1)}} \left(\frac{\frac{2}{N_F}\prod_{\substack{n_1,n_2=1\\n_2>n_1}}^{N_F}\left(\frac{(-\hat{\eta}_{n_1n_2m}^{u-})\sqrt{P_{u,n_1}P_{u,n_2}}}{\theta_{n_1n_2mu}^{(2)}}\right)^{\theta_{n_1n_2mu}^{(2)}}}{\tau_{um}^{(2)}}\right)^{\tau_{um}^{(2)}} \tag{43}$$

$$\tau_{um}^{(1)} = \frac{\delta_u \prod_{l=1}^{N_F}\left(\frac{P_{u,l}}{\theta_{ul}^{(1)}}\right)^{\theta_{ul}^{(1)}}}{\delta_u \prod_{l=1}^{N_F}\left(\frac{P_{u,l}}{\theta_{ul}^{(1)}}\right)^{\theta_{ul}^{(1)}} + \frac{2}{N_F}\prod_{\substack{n_1,n_2=1\\n_2>n_1}}^{N_F}\left(\frac{(-\hat{\eta}_{n_1n_2m}^{u-})\sqrt{P_{u,n_1}P_{u,n_2}}}{\theta_{n_1n_2mu}^{(2)}}\right)^{\theta_{n_1n_2mu}^{(2)}}}$$

$$\tau_{um}^{(2)} = \frac{\frac{2}{N_F}\prod_{\substack{n_1,n_2=1\\n_2>n_1}}^{N_F}\left(\frac{(-\hat{\eta}_{n_1n_2m}^{u-})\sqrt{P_{u,n_1}P_{u,n_2}}}{\theta_{n_1n_2mu}^{(2)}}\right)^{\theta_{n_1n_2mu}^{(2)}}}{\delta_u \prod_{l=1}^{N_F}\left(\frac{P_{u,l}}{\theta_{ul}^{(1)}}\right)^{\theta_{ul}^{(1)}} + \frac{2}{N_F}\prod_{\substack{n_1,n_2=1\\n_2>n_1}}^{N_F}\left(\frac{(-\hat{\eta}_{n_1n_2m}^{u-})\sqrt{P_{u,n_1}P_{u,n_2}}}{\theta_{n_1n_2mu}^{(2)}}\right)^{\theta_{n_1n_2mu}^{(2)}}} \tag{45}$$

$$\sum_{l=1}^{N_F}(\kappa^u + 2d_l^u)P_{u,l} + \frac{2}{N_F}\sum_{\substack{n_1,n_2=1\\n_2>n_1}}^{N_F}\hat{\eta}_{n_1n_2m}^{u+}\sqrt{P_{u,n_1}P_{u,n_2}} \leq$$
$$\left(\frac{\delta_u \prod_{l=1}^{N_F}\left(\frac{P_{u,l}}{\theta_{ul}^{(1)}}\right)^{\theta_{ul}^{(1)}}}{\tau_{um}^{(1)}}\right)^{\tau_{um}^{(1)}} \left(\frac{\frac{2}{N_F}\prod_{\substack{n_1,n_2=1\\n_2>n_1}}^{N_F}\left(\frac{(-\hat{\eta}_{n_1n_2m}^{u-})\sqrt{P_{u,n_1}P_{u,n_2}}}{\theta_{n_1n_2mu}^{(2)}}\right)^{\theta_{n_1n_2mu}^{(2)}}}{\tau_{um}^{(2)}}\right)^{\tau_{um}^{(2)}} \tag{46}$$

---

where $\hat{T}_m(\boldsymbol{\alpha}_u, \hat{\boldsymbol{\alpha}}_u)$ is given in (39), $T_m(\boldsymbol{\alpha}_u)$ is the RHS of (25) after change of variables (COV), and the partial derivatives are given as

$$\frac{\partial T_m}{\partial \alpha_{u,k}} = \delta_u e^{\alpha_{u,k}} + \frac{1}{2}\sum_{n=k+1}^{N_F}(-\tilde{d}_{mkn}^{u-})e^{\frac{1}{2}(\alpha_{u,k}+\alpha_{u,n})} + \frac{1}{2}\sum_{n=1}^{k-1}(-\tilde{d}_{mnk}^{u-})e^{\frac{1}{2}(\alpha_{u,n}+\alpha_{u,k})}. \tag{52}$$

Appendix F
SCAGP for PAPR constraint in OFDMA

Applying [6, Eq. (36)] to RHS of (25) yields a constraint (53). where

$$\theta_{ul}^{(1)} = \frac{P_{u,l}}{\sum_{l'=1}^{N_F} P_{u,l'}},$$
$$\theta_{mn_2n_1u}^{(2)} = \frac{-\tilde{d}_{mn_2n_1}^{u-}\sqrt{P_{u,n_1}P_{u,n_2}}}{\sum_{\substack{n_1',n_2'=1\\n_2'>n_1'}}^{N_F} -\tilde{d}_{mn_2'n_1'}^{u-}\sqrt{P_{u,n_1'}P_{u,n_2'}}}, \tag{54}$$

and $\tau_{um}^{(1)}$ and $\tau_{um}^{(2)}$ are given in (55). Hence, constraint (25) can be approximated $\forall u, m$ using SCA with (53). The LHS is a posynomial and RHS is a monomial and hence, (53) is a valid GP constraint.

Appendix G
Power variance constraint for SC-FDMA

Let the average power of the transmitted signal of the u^{th} user be denoted as $\mu_u = \frac{1}{N_F}\sum_{l=1}^{N_F} P_{u,l}$. Assuming $\mathbb{E}\{|b_n^u|\} = 1, \forall u, n$ and $\mathbb{E}\{b_{n_1}^u b_{n_2}^{u*}\} = 0, \forall n_1 \neq n_2$, the variance of the output power is given by

$$\Sigma^2(\mathbf{P}_u) = \frac{1}{N_F}\sum_{k=1}^{N_F}(\mathbb{E}[|s_k^u|^4] - \mu_u^2)$$
$$= \frac{1}{N_F}\sum_{k=1}^{N_F}[2(\sum_{m=1}^{N_F}|g_{k,m}^u|^2)^2 - \sum_{m=1}^{N_F}|g_{k,m}^u|^4] - \mu_u^2. \tag{56}$$

The first term reduces to

$$\frac{1}{N_F}\sum_{k=1}^{N_F}(\sum_{m=1}^{N_F}|g_{k,m}^u|^2)^2 = \mu_u^2. \tag{57}$$

The second term can be expressed as a function of power allocation as

$$\frac{1}{N_F}\sum_{k=1}^{N_F}\sum_{m=1}^{N_F}|g_{k,m}^u|^4 = \frac{\mu_u^2}{N_F} + \frac{1}{N_F^3}\sum_{n_1,n_2\in\mathcal{S}_1}^{N_F}P_{u,n_1}P_{u,n_2} + \frac{1}{N_F^3}\sum_{n_1,n_2,n_3,n_4\in\mathcal{S}_2}^{N_F}\sqrt{P_{u,n_1}P_{u,n_2}P_{u,n_3}P_{u,n_4}}, \tag{58}$$

where $\mathcal{S}_1 = \Big\{n_1, n_2 \in \{1, 2, \ldots, N_F\} : n_1 \neq n_2, n_1 - n_2 = \pm N_F/2\Big\}$ and $\mathcal{S}_2 = \Big\{n_1, n_2, n_3, n_4 \in \{1, 2, \ldots, N_F\} : n_1 \neq n_2, n_3 \neq n_4, (n_1, n_2) \neq (n_3, n_4), n_4 - n_3 \in \{n_1 - n_2, N_F + n_1 - n_2, -N_F + n_1 - n_2\}\Big\}$. Substituting (57) and (58) in (56)

$$\sum_{l=1}^{N_F}|b_l^u|^2P_{u,l}+\sum_{\substack{n_1,n_2=1\\n_2>n_1}}^{N_F}\tilde{d}^{u+}_{mn_2n_1}\sqrt{P_{u,n_1}P_{u,n_2}}\le\left(\frac{\delta_u\prod_{l=1}^{N_F}\left(\frac{P_{u,l}}{\theta^{(1)}_{ul}}\right)^{\theta^{(1)}_{ul}}}{\tau^{(1)}_{um}}\right)^{\tau^{(1)}_{um}}\left(\frac{\prod_{\substack{n_1,n_2=1\\n_2>n_1}}^{N_F}\left(\frac{(-\tilde{d}^{u-}_{mn_2n_1})\sqrt{P_{u,n_1}P_{u,n_2}}}{\theta^{(2)}_{mn_2n_1u}}\right)^{\theta^{(2)}_{mn_2n_1u}}}{\tau^{(2)}_{um}}\right)^{\tau^{(2)}_{um}} \tag{53}$$

$$\begin{aligned}\tau^{(1)}_{um}&=\frac{\delta_u\prod_{l=1}^{N_F}\left(\frac{P_{u,l}}{\theta^{(1)}_{ul}}\right)^{\theta^{(1)}_{ul}}}{\delta_u\prod_{l=1}^{N_F}\left(\frac{P_{u,l}}{\theta^{(1)}_{ul}}\right)^{\theta^{(1)}_{ul}}+\prod_{\substack{n_1,n_2=1\\n_2>n_1}}^{N_F}\left(\frac{(-\tilde{d}^{u-}_{mn_2n_1})\sqrt{P_{u,n_1}P_{u,n_2}}}{\theta^{(2)}_{mn_2n_1u}}\right)^{\theta^{(2)}_{mn_2n_1u}}}\\ \tau^{(2)}_{um}&=\frac{\prod_{\substack{n_1,n_2=1\\n_2>n_1}}^{N_F}\left(\frac{(-\tilde{d}^{u-}_{mn_2n_1})\sqrt{P_{u,n_1}P_{u,n_2}}}{\theta^{(2)}_{mn_2n_1u}}\right)^{\theta^{(2)}_{mn_2n_1u}}}{\delta_u\prod_{l=1}^{N_F}\left(\frac{P_{u,l}}{\theta^{(1)}_{ul}}\right)^{\theta^{(1)}_{ul}}+\prod_{\substack{n_1,n_2=1\\n_2>n_1}}^{N_F}\left(\frac{(-\tilde{d}^{u-}_{mn_2n_1})\sqrt{P_{u,n_1}P_{u,n_2}}}{\theta^{(2)}_{mn_2n_1u}}\right)^{\theta^{(2)}_{mn_2n_1u}}}\end{aligned} \tag{55}$$

we get

$$\Sigma^2(\mathbf{P}_u)=\frac{N_F-1}{N_F^3}(\sum_{l=1}^{N_F}P_{u,l})^2-\frac{1}{N_F^3}\sum_{n_1,n_2\in\mathcal{S}_1}^{N_F}P_{u,n_1}P_{u,n_2}-\frac{1}{N_F^3}\sum_{n_1,n_2,n_3,n_4\in\mathcal{S}_2}^{N_F}\sqrt{P_{u,n_1}P_{u,n_2}P_{u,n_3}P_{u,n_4}}. \tag{59}$$

The number of summation terms in $\sum_{n_1,n_2,n_3,n_4\in\mathcal{S}_2}^{N_F}$ is $N_F^3-N_F^2-N_F$. Hence, the number of summation terms in (59) increases in the order of $N_F^3-N_F^2+N_F$. The objective is to control the variance of the normalized power, and hence $P_{u,l}$ in (59) is divided by $\sum_{n=1}^{N_F}P_{u,n}$, $\forall l$. Hence, the constraint for power variance is written as

$$\Sigma^2(\mathbf{P}_u)\le\tilde{\sigma}_u^2(\sum_{l=1}^{N_F}P_{u,l})^2, \tag{60}$$

where $\tilde{\sigma}_u^2\in\mathbb{R}^+$ is the preset upper bound of the variance of transmitted power for the u^{th} user. Plugging (59) into (60) the constraint can be written as

$$(N_F-1)(\sum_{l=1}^{N_F}P_{u,l})^2\le\sum_{n_1,n_2\in\mathcal{S}_1}^{N_F}P_{u,n_1}P_{u,n_2}+\sum_{n_1,n_2,n_3,n_4\in\mathcal{S}_2}^{N_F}\sqrt{P_{u,n_1}P_{u,n_2}P_{u,n_3}P_{u,n_4}}+(\sum_{l=1}^{N_F}P_{u,l})^2\tilde{\sigma}_u^2N_F^3. \tag{61}$$

Appendix H
SCACOV for power variance constraint in SC-FDMA

Changing the variables as $P_{u,m}=e^{\alpha_{u,m}}$, $\forall u,m$, both LHS and RHS of (26) are convex functions. The linear upper bound of the convex RHS is approximated a convex constraint

$$(N_F-1)(\sum_{l=1}^{N_F}e^{\alpha_{u,l}})^2\le\hat{T}(\boldsymbol{\alpha}_u,\hat{\boldsymbol{\alpha}}_u), \tag{62}$$

where $\hat{T}(\boldsymbol{\alpha}_u,\hat{\boldsymbol{\alpha}}_u)$ is given in (39), $T(\hat{\boldsymbol{\alpha}}_u)$ is the RHS of (26) after change of variables, and the partial derivatives are given as

$$\begin{aligned}\frac{\partial T}{\partial\alpha_{u,k}}=&2\sum_{\substack{n=1\\n\neq k\\n-k=\pm N_F/2}}^{N_F}e^{\alpha_{u,n}+\alpha_{u,k}}+\\&2\sum_{\substack{n_1,n_2,n_3=1\\n_1\neq n_2,n_3\neq k\\(n_1,n_2)\neq(n_3,k)\\k-n_3\in\mathcal{S}}}^{N_F}e^{\frac{1}{2}(\alpha_{u,n_1}+\alpha_{u,n_2}+\alpha_{u,n_3}+\alpha_{u,k})}\\&+2\tilde{\sigma}_u^2N_F^3(\sum_{l=1}^{N_F}e^{\alpha_{u,l}+\alpha_{u,k}})^2,\end{aligned} \tag{63}$$

where $\mathcal{S}=\{n_1-n_2,N_F+n_1-n_2,-N_F+n_1-n_2\}$.

Appendix I
SCAGP for power variance constraint in SC-FDMA

Similarly to Appendix C, applying [6, Eq. (36)] to the RHS of (26) yields a constraint (64), where the weights are given in (65) and

$$\begin{aligned}\theta^{(1)}_{un_1n_2}&=\frac{P_{u,n_1}P_{u,n_2}}{\sum_{n_1',n_2'\in\mathcal{S}_1}P_{u,n_1'}P_{u,n_2'}},\\ \theta^{(2)}_{un_1n_2n_3n_4}&=\frac{\sqrt{P_{u,n_1}P_{u,n_2}P_{u,n_3}P_{u,n_4}}}{\sum_{n_1',n_2',n_3',n_4'\in\mathcal{S}_2}\sqrt{P_{un_1'}P_{u,n_2'}P_{u,n_3'}P_{u,n_4'}}},\\ \theta^{(3)}_{ul}&=\frac{P_{u,l}^2}{\sum_{l'=1}^{N_F}P_{u,l'}^2},\quad\theta^{(4)}_{un_1n_2}=\frac{P_{u,n_1}P_{u,n_2}}{\sum_{\substack{n_1',n_2'=1\\n_2'>n_1'}}^{N_F}P_{u,n_1'}P_{u,n_2'}}.\end{aligned} \tag{66}$$

Appendix J
Power variance constraint for OFDMA

In the case of OFDMA, the first term of (56) reduces to

$$\frac{1}{N_F}\sum_{k=1}^{N_F}(\sum_{m=1}^{N_F}|g^u_{k,m}|^2)^2=2\mu_u^2, \tag{67}$$

$$
(N_F-1)(\sum_{l=1}^{N_F}P_{u,l})^2 \le \left(\frac{\prod_{n_1,n_2\in\mathcal{S}_1}\left(\frac{P_{u,n_1}P_{u,n_2}}{\theta^{(1)}_{un_1n_2}}\right)^{\theta^{(1)}_{un_1n_2}}}{\tau_u^{(1)}}\right)^{\tau_u^{(1)}}\left(\frac{2\tilde{\sigma}_u^2N_F^3\prod_{\substack{n_1,n_2=1\\n_2>n_1}}^{N_F}\left(\frac{P_{u,n_1}P_{u,n_2}}{\theta^{(4)}_{un_1n_2}}\right)^{\theta^{(4)}_{un_1n_2}}}{\tau_u^{(4)}}\right)^{\tau_u^{(4)}}
$$
$$
\times\left(\frac{\prod_{n_1,n_2,n_3,n_4\in\mathcal{S}_2}\left(\frac{\sqrt{P_{u,n_1}P_{u,n_2}P_{u,n_3}P_{u,n_4}}}{\theta^{(2)}_{un_1n_2n_3n_4}}\right)^{\theta^{(2)}_{un_1n_2n_3n_4}}}{\tau_u^{(2)}}\right)^{\tau_u^{(2)}}\left(\frac{\tilde{\sigma}_u^2N_F^3\prod_{l=1}^{N_F}\left(\frac{P_{u,l}^2}{\theta^{(3)}_{ul}}\right)^{\theta^{(3)}_{ul}}}{\tau_u^{(3)}}\right)^{\tau_u^{(3)}} \quad (64)
$$

$$
\begin{aligned}
\tau_u^{(1)} =& \frac{\sum_{n_1,n_2\in\mathcal{S}_1}P_{u,n_1}P_{u,n_2}}{\sum_{n_1,n_2\in\mathcal{S}_1}P_{u,n_1}P_{u,n_2}+\sum_{n_1,n_2,n_3,n_4\in\mathcal{S}_2}\sqrt{P_{u,n_1}P_{u,n_2}P_{u,n_3}P_{u,n_4}}+(\sum_{l=1}^{N_F}P_{u,l})^2\tilde{\sigma}_u^2N_F^3}\\
\tau_u^{(2)} =& \frac{\sum_{n_1,n_2,n_3,n_4\in\mathcal{S}_2}\sqrt{P_{u,n_1}P_{u,n_2}P_{u,n_3}P_{u,n_4}}}{\sum_{n_1,n_2\in\mathcal{S}_1}P_{u,n_1}P_{u,n_2}+\sum_{n_1,n_2,n_3,n_4\in\mathcal{S}_2}\sqrt{P_{u,n_1}P_{u,n_2}P_{u,n_3}P_{u,n_4}}+(\sum_{l=1}^{N_F}P_{u,l})^2\tilde{\sigma}_u^2N_F^3}\\
\tau_u^{(3)} =& \frac{\tilde{\sigma}_u^2N_F^3\sum_{l=1}^{N_F}P_{u,l}^2}{\sum_{n_1,n_2\in\mathcal{S}_1}P_{u,n_1}P_{u,n_2}+\sum_{n_1,n_2,n_3,n_4\in\mathcal{S}_2}\sqrt{P_{u,n_1}P_{u,n_2}P_{u,n_3}P_{u,n_4}}+(\sum_{l=1}^{N_F}P_{u,l})^2\tilde{\sigma}_u^2N_F^3}\\
\tau_u^{(4)} =& \frac{2\tilde{\sigma}_u^2N_F^3\sum_{\substack{n_1,n_2=1\\n_2>n_1}}^{N_F}P_{u,n_1}P_{u,n_2}}{\sum_{n_1,n_2\in\mathcal{S}_1}P_{u,n_1}P_{u,n_2}+\sum_{n_1,n_2,n_3,n_4\in\mathcal{S}_2}\sqrt{P_{u,n_1}P_{u,n_2}P_{u,n_3}P_{u,n_4}}+(\sum_{l=1}^{N_F}P_{u,l})^2\tilde{\sigma}_u^2N_F^3}
\end{aligned} \quad (65)
$$

while the second term is simplified to

$$
\frac{1}{N_F}\sum_{k=1}^{N_F}\sum_{m=1}^{N_F}|g^u_{k,m}|^4 = \frac{1}{N_F^2}\sum_{m=1}^{N_F}P_{u,m}^2. \quad (68)
$$

Substituting (67) and (68) in (56) we get

$$
\Sigma^2(\mathbf{P}_u) = \frac{2}{N_F^2}\sum_{\substack{n_1,n_2=1\\n_2>n_1}}^{N_F}P_{u,n_2}P_{u,n_1}. \quad (69)
$$

The summation terms in (69) increases in the order of $N_F(N_F-1)-\sum_{n=1}^{N_F}n$. After normalization, the variance constraint is written as

$$
\frac{2}{N_F^2}\sum_{\substack{n_1,n_2=1\\n_2>n_1}}^{N_F}P_{u,n_2}P_{u,n_1} \le \tilde{\sigma}_u^2\left(\sum_{m=1}^{N_F}P_{u,m}\right)^2. \quad (70)
$$

Appendix K
SCACOV for power variance constraint in OFDMA

Changing the variables to $P_{u,m}=e^{\alpha_{u,m}}$, $\forall u,m$, constraint (27) can be approximated as

$$
\frac{2}{N_F^2}\sum_{\substack{n_1,n_2=1\\n_2>n_1}}^{N_F}e^{\alpha_{u,n_2}+\alpha_{u,n_1}} \le \hat{T}(\boldsymbol{\alpha}_u,\hat{\boldsymbol{\alpha}}_u), \quad (71)
$$

where $\hat{T}(\boldsymbol{\alpha}_u,\hat{\boldsymbol{\alpha}}_u)$ is given in (39), $T(\hat{\boldsymbol{\alpha}}_u)$ is the RHS of (26) after COV, and the partial derivatives are given as $\frac{\partial T}{\partial \alpha_{u,k}} = 2\tilde{\sigma}_u^2\sum_{m=1}^{N_F}e^{\alpha_{u,m}+\alpha_{u,k}}$.

Appendix L
SCAGP for power variance constraint in OFDMA

Applying [6, Eq. (36)] to the RHS of (27) yields a constraint (72), where the weights are given in

$$
\tau_u^{(1)} = \frac{\prod_{m=1}^{N_F}\left(\frac{P_{u,m}^2}{\theta^{(1)}_{um}}\right)^{\theta^{(1)}_{um}}}{\prod_{m=1}^{N_F}\left(\frac{P_{u,m}^2}{\theta^{(1)}_{um}}\right)^{\theta^{(1)}_{um}}+2\prod_{\substack{n_1,n_2=1^N\\n_2>n_1\ \ F}}\left(\frac{P_{u,n_1}P_{u,n_2}}{\theta^{(2)}_{un_1n_2}}\right)^{\theta^{(2)}_{un_1n_2}}}
$$
$$
\tau_u^{(2)} = \frac{2\prod_{\substack{n_1,n_2=1^N\\n_2>n_1\ \ F}}\left(\frac{P_{u,n_1}P_{u,n_2}}{\theta^{(2)}_{un_1n_2}}\right)^{\theta^{(2)}_{un_1n_2}}}{\prod_{m=1}^{N_F}\left(\frac{P_{u,m}^2}{\theta^{(1)}_{um}}\right)^{\theta^{(1)}_{um}}+2\prod_{\substack{n_1,n_2=1^N\\n_2>n_1\ \ F}}\left(\frac{P_{u,n_1}P_{u,n_2}}{\theta^{(2)}_{un_1n_2}}\right)^{\theta^{(2)}_{un_1n_2}}}, \quad (73)
$$

and

$$
\theta^{(1)}_{un_1} = \frac{P_{u,n_1}^2}{\sum_{n_1'=1}^{N_F}},\quad \theta^{(2)}_{un_1n_2} = \frac{P_{u,n_1}P_{u,n_2}}{\sum_{\substack{n_1',n_2'=1\\n_2'>n_1'}}^{N_F}P_{u,n_1'}P_{u,n_2'}}. \quad (74)
$$

References

[1] F. Pancaldi, G. Vitetta, R. Kalbasi, N. Al-Dhahir, M. Uysal, and H. Mheidat, "Single-carrier frequency domain equalization," *IEEE Signal Processing Mag.*, vol. 25, no. 5, pp. 37–56, 2008.

[2] 3rd Generation Partnership Project (3GPP); Technical Specification Group Radio Access Network Evolved Universal Terrestrial Radio Access E-UTRA, "Physical channels and modulation 3GPP TS 36.211 Version 12.1.0 (Release 12)," Tech. Rep., 2014.

[3] R. V. Nee and R. Prasad, *OFDM for Wireless Multimedia Communications*. Norwood, MA: Artech House, 2000.

[4] D. Tse and P. Viswanath, *Fundamentals of Wireless Communication*. Cambridge, U.K.: Cambridge Univ. Press, 2005.

[5] J. Karjalainen, M. Codreanu, A. Tölli, M. Juntti, and T. Matsumoto, "EXIT chart-based power allocation for iterative frequency domain MIMO detector," *IEEE Trans. Signal Processing*, vol. 59, no. 4, pp. 1624–1641, Apr. 2011.

[6] V. Tervo, A. Tölli, J. Karjalainen, and T. Matsumoto, "Convergence constrained multiuser transmitter-receiver optimization in single carrier FDMA," *IEEE Trans. Signal Processing*, vol. 63, no. 6, pp. 1500–1511, 2015.

$$\frac{2}{N_F^2}\sum_{\substack{n_1,n_2=1\\ n_2>n_1}}^{N_F} P_{u,n_2}P_{u,n_1} \leq \left(\frac{\prod_{m=1}^{N_F}\left(\frac{P_{u,m}^2}{\theta_{um}^{(1)}}\right)^{\theta_{um}^{(1)}}}{\tau_u^{(1)}}\right)^{\tau_u^{(1)}} \left(\frac{2\prod_{\substack{n_1,n_2=1\\ n_2>n_1}}^{N_F}\left(\frac{P_{u,n_1}P_{u,n_2}}{\theta_{un_1n_2}^{(2)}}\right)^{\theta_{un_1n_2}^{(2)}}}{\tau_u^{(2)}}\right)^{\tau_u^{(2)}} \quad (72)$$

[7] G. Wunder, R. Fischer, H. Boche, S. Litsyn, and J.-S. No, "The PAPR problem in OFDM transmission: New directions for a long-lasting problem," *IEEE Signal Processing Mag.*, vol. 30, no. 6, pp. 130–144, Nov 2013.

[8] J. Tellado, "Peak to average power reduction for multicarrier modulation," Ph.D. dissertation, Stanford Univ., 2000.

[9] S. H. Han and J. H. Lee, "An overview of peak-to-average power ratio reduction techniques for multicarrier transmission," *IEEE Wireless Commun. Mag.*, vol. 12, no. 2, pp. 56–65, April 2005.

[10] R. Bäuml, R. Fischer, and J. Huber, "Reducing the peak-to-average power ratio of multicarrier modulation by selected mapping," *IEE Electron. Lett.*, vol. 32, no. 22, pp. 2056–2057, 1996.

[11] S. Müller and J. Huber, "OFDM with reduced peak-to-average power ratio by optimum combination of partial transmit sequences," *IEE Electron. Lett.*, vol. 33, no. 5, pp. 368–369, Feb. 1997.

[12] A. Alavi, C. Tellambura, and I. Fair, "PAPR reduction of OFDM signals using partial transmit sequence: an optimal approach using sphere decoding," *IEEE Commun. Lett.*, vol. 9, no. 11, pp. 982–984, Nov 2005.

[13] H.-K.-C. Kwok and D. Jones, "PAR reduction for Hadamard transform based OFDM," in *Proc. Conf. Inform. Sciences Syst. (CISS)*, Princeton, NJ, Mar. 2000.

[14] A. Mobasher and A. Khandani, "Integer-based constellation-shaping method for PAPR reduction in OFDM systems," *IEEE Trans. Commun.*, vol. 54, no. 1, pp. 119–127, Jan 2006.

[15] C. Eugen, D. Sterian, and K. Wesolowski, "Reducing the peak and average power for OFDM systems using QAM by constellation shaping," *European Trans. Telecommun.*, vol. 21, no. 1, pp. 35–49, Jan 2010.

[16] S. Slimane, "Reducing the peak-to-average power ratio of OFDM signals through precoding," *IEEE Trans. Veh. Technol.*, vol. 56, no. 2, pp. 686–695, 2007.

[17] D. Falconer, "Linear precoding of OFDMA signals to minimize their instantaneous power variance," *IEEE Trans. Commun.*, vol. 59, no. 4, pp. 1154–1162, 2011.

[18] C. Yuen and B. Farhang-Boroujeny, "Analysis of the optimum precoder in SC-FDMA," *IEEE Trans. Wireless Commun.*, vol. 11, no. 11, pp. 4096–4107, 2012.

[19] B. R. Marks and G. P. Wright, "A general inner approximation algorithm for nonconvex mathematical programs," *Journal of the Operations Research Society of America*, vol. 26, no. 4, pp. 681–683, Jul–Aug 1978.

[20] J. Kaleva, A. Tölli, G. Venkatraman, and M. Juntti, "Downlink precoder design for coordinated regenerative multi-user relaying," *IEEE Trans. Signal Processing*, vol. 61, no. 5, pp. 1215–1229, March 2013.

[21] M. Chiang, C. wei Tan, D. Palomar, D. O'Neill, and D. Julian, "Power control by geometric programming," *IEEE Trans. Wireless Commun.*, vol. 6, no. 7, pp. 2640–2651, 2007.

[22] V. Tervo, A. Tölli, J. Karjalainen, and T. Matsumoto, "PAPR constrained power allocation for iterative frequency domain multiuser SIMO detector," in *Proc. IEEE Int. Conf. Commun.*, Sydney, Australia, Jun.10–14 2014, pp. 4735–4740.

[23] ——, "Transmission power variance constrained power allocation for iterative frequency domain multiuser simo detector," in *Proc. IEEE Int. Conf. Acoust., Speech, Signal Processing*, May 2014, pp. 3493–3497.

[24] J. Karjalainen, "Broadband single carrier multi-antenna communications with frequency domain turbo equalization," Ph.D. dissertation, University of Oulu, Oulu, Finland, 2011. [Online]. Available: http://herkules.oulu.fi/isbn9789514295027/isbn9789514295027.pdf

[25] S. Boyd and L. Vandenberghe, *Convex Optimization*. Cambridge, U.K.: Cambridge Univ. Press, 2004.

[26] D. Divsalar, H. Jin, and R. J. McEliece, "Coding theorems for 'turbo-like' codes," in *Proc. Annual Allerton Conf. Commun., Contr., Computing*, Urbana, Illinois, USA, Sep.23–25 1998, pp. 201–210.

[27] S. ten Brink, "Convergence behavior of iteratively decoded parallel concatenated codes," *IEEE Trans. Commun.*, vol. 49, no. 10, pp. 1727–1737, Oct. 2001.

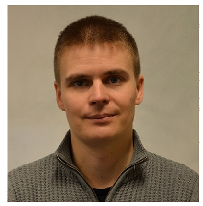

Valtteri Tervo (S'10, M'15) received the Dr.Sc (Tech.) degree in Telecommunications from the University of Oulu, Finland in February 2015. He pursued his doctoral degree under the dual degree program between the University of Oulu and Japan Advanced Institute of Science and Technology (JAIST) which resulted in a Ph.D. degree from JAIST in March 2015 with Outstanding Performance Award. From the beginning of 2015, V. Tervo has been working as a work package leader in FP7 project Links-on-the-fly Technology for Robust, Efficient and Smart Communication in Unpredictable Environments (RESCUE). His research interests are in power allocation and transceiver design for broadband wireless communications with special emphasis on iterative reception. His research activities also include physical and lower MAC layer algorithms, including error correction code design and optimization, in lossy decode-and-forward relay networks.

Antti Tölli (M'08, SM'14) received the Dr.Sc. (Tech.) degree in electrical engineering from the University of Oulu, Oulu, Finland, in 2008. Before joining the Department of Communication Engineering (DCE) and Centre for Wireless Communications (CWC) at the University of Oulu, he worked for 5 years with Nokia Networks, IP Mobility Networks Division, as a Research Engineer and Project Manager both in Finland and Spain. In May 2014, he was granted a five year (2014–2019) Academy Research Fellow post by the Research Council for Natural Sciences and Engineering of the Academy of Finland. He also holds an Adjunct Professor position with the DCE, University of Oulu. During the academic year 2015-2016, he holds a visiting position at EURECOM, Sophia Antipolis, France. He has authored more than 120 papers in peer-reviewed international journals and conferences and several patents all in the area of signal processing and wireless communications. His research interests include radio resource management and transceiver design for broadband wireless communications with a special emphasis on distributed interference management in heterogeneous wireless networks. He served as the General Co-Chair of IEEE WDN in 2010 and 2011, as well as Finance Chair of IEEE CTW 2011. He is also chairing the Workshop on Novel Medium Access and Resource Allocation for 5G Networks held in conjunction with IEEE ICC'16.

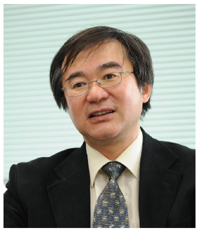

Tad Matsumoto (S'84-SM'95-F'10) received the B.S., M.S., and Ph.D. degrees from Keio University, Yokohama, Japan, in 1978, 1980, and 1991, respectively, all in electrical engineering. He joined Nippon Telegraph and Telephone Corporation (NTT) in April 1980. Since he engaged in NTT, he was involved in a lot of research and development projects, all for mobile wireless communications systems. In July 1992, he transferred to NTT DoCoMo, where he researched Code-Division Multiple-Access techniques for Mobile Communication Systems. In April 1994, he transferred to NTT America, where he served as a Senior Technical Advisor of a joint project between NTT and NEXTEL Communications. In March 1996, he returned to NTT DoCoMo, where he served as a Head of the Radio Signal Processing Laboratory until August of 2001. He worked on adaptive signal processing, multiple-input multiple-output turbo signal detection, interference cancellation, and space-time coding techniques for broadband mobile communications. In March 2002, he moved to University of Oulu, Finland, where he served as a Professor at the Centre for Wireless Communications. In 2006, he served as a Visiting Professor at Ilmenau University of Technology, Ilmenau, Germany, funded by the German MERCATOR Visiting Professorship Program. Since April 2007, he has been serving as a Professor at the Japan Advanced Institute of Science and Technology (JAIST), Japan, while also keeping the position at University of Oulu. He was appointed a Finland Distinguished Professor for a period from January 2008 to December 2012, funded by the Finnish National Technology Agency (Tekes) and Finnish Academy, under which he preserves the rights to participate in and apply to European and Finnish national projects. He is a recipient of the IEEE VTS Outstanding Service Award (2001), Nokia Foundation Visiting Fellow Scholarship Award (2002), IEEE Japan Council Award for Distinguished Service to the Society (2006), IEEE Vehicular Technology Society James R. Evans Avant Garde Award (2006), and Thuringen State Research Award for Advanced Applied Science (2006), 2007 Best Paper Award of Institute of Electrical, Communication, and Information Engineers of Japan (2008), Telecom System Technology Award by the Telecommunications Advancement Foundation (2009), IEEE Communication Letters Exemplifying Reviewer Award (2011), and Nikkei Wireless Japan Award (2012). He is a member of IEICE. He has been serving as an IEEE Vehicular Technology Distinguished Lecturer during the term July 2011-June 2015.